









Article

Discovery of Trace Amine-Associated Receptor 1 (TAAR1) Agonist 2-(5-(4'-Chloro-[1,1'-biphenyl]-4-yl)-4H-1,2,4-triazol-3-yl)ethan-1-amine (LK00764) for the Treatment of Psychotic Disorders

Mikhail Krasavin ^{1,2,*}, Alexey Lukin ³, Ilya Sukhanov ⁴ , Andrey S. Gerasimov ⁵ , Savelii Kuvarzin ⁵ , Evgeniya V. Efimova ⁵ , Mariia Dorofeikova ⁶ , Anna Nichugovskaya ³, Andrey Matveev ³ , Kirill Onokhin ^{5,6}, Konstantin Zakharov ⁶ , Maxim Gureev ⁷  and Raul R. Gainetdinov ^{5,*}

- ¹ Department of Medicinal Chemistry, Institute of Chemistry, Saint Petersburg State University, 199034 Saint Petersburg, Russia
² Institute for Medicine and Life Sciences, Immanuel Kant Baltic Federal University, 236041 Kaliningrad, Russia
³ Lomonosov Institute of Fine Chemical Technologies, MIREA—Russian Technological University, 119454 Moscow, Russia
⁴ Valdman Institute of Pharmacology, Pavlov First Saint Peterburg State Medical University, 197022 Saint Petersburg, Russia
⁵ Institute of Translational Biomedicine, Saint Petersburg State University, 199034 Saint Petersburg, Russia
⁶ Accellena Research and Development Inc., 88A Sredniy pr. V.O., 199106 Saint Petersburg, Russia
⁷ Center of Bio- and Chemoinformatics, I.M. Sechenov First Moscow State Medical University, 119991 Moscow, Russia
* Correspondence: mkrasavin@spbu.ru (M.K.); gainetdinov.raul@gmail.com (R.R.G.)



Citation: Krasavin, M.; Lukin, A.; Sukhanov, I.; Gerasimov, A.S.; Kuvarzin, S.; Efimova, E.V.; Dorofeikova, M.; Nichugovskaya, A.; Matveev, A.; Onokhin, K.; et al. Discovery of Trace Amine-Associated Receptor 1 (TAAR1) Agonist 2-(5-(4'-Chloro-[1,1'-biphenyl]-4-yl)-4H-1,2,4-triazol-3-yl)ethan-1-amine (LK00764) for the Treatment of Psychotic Disorders. *Biomolecules* **2022**, *12*, 1650. <https://doi.org/10.3390/biom12111650>

Academic Editor: Philippe De Deurwaerdère

Received: 5 October 2022

Accepted: 2 November 2022

Published: 7 November 2022

Publisher's Note: MDPI stays neutral with regard to jurisdictional claims in published maps and institutional affiliations.



Copyright: © 2022 by the authors. Licensee MDPI, Basel, Switzerland. This article is an open access article distributed under the terms and conditions of the Creative Commons Attribution (CC BY) license (<https://creativecommons.org/licenses/by/4.0/>).

Abstract: A focused in-house library of about 1000 compounds comprising various heterocyclic motifs in combination with structural fragments similar to β -phenylethylamine or tyramine was screened for the agonistic activity towards trace amine-associated receptor 1 (TAAR1). The screening yielded two closely related hits displaying EC₅₀ values in the upper submicromolar range. Extensive analog synthesis and testing for TAAR1 agonism in a BRET-based cellular assay identified compound **62** (LK00764) with EC₅₀ = 4.0 nM. The compound demonstrated notable efficacy in such schizophrenia-related in vivo tests as MK-801-induced hyperactivity and spontaneous activity in rats, locomotor hyperactivity of dopamine transporter knockout (DAT-KO) rats, and stress-induced hyperthermia (i.p. administration). Further preclinical studies are necessary to evaluate efficacy, safety and tolerability of this potent TAAR1 agonist for the potential development of this compound as a new pharmacotherapy option for schizophrenia and other psychiatric disorders.

Keywords: schizophrenia; trace amine-associated receptor 1; agonism; 1,2,4-triazoles; dopamine transporter knockout rats; dopamine; MK-801-induced hyperactivity; spontaneous activity; locomotor hyperactivity; stress-induced hyperthermia

1. Introduction

Schizophrenia is a chronic debilitating psychiatric disorder affecting about 1% of the human population worldwide. Schizophrenia is characterized by a complex set of abnormal mental manifestations, such as positive and negative symptoms as well as cognitive deficits [1]. Antipsychotics, that have commonly been used for the treatment of schizophrenia symptoms since their discovery in the 1950s, are categorized as typical or atypical. All clinically effective antipsychotics have a common mechanism of action involving the blockade of D₂ dopamine receptors; however, the typical ones are more potent dopamine D₂ receptor antagonists and, thus, cause more pronounced side effects such as hyperprolactinemia and extrapyramidal symptoms (EPS). Atypical antipsychotic drugs, in

addition to the blockade of dopamine D₂ receptors, also display antagonism at serotonin 5-HT_{2A} receptors and are often associated with an increased risk for metabolic symptoms such as weight gain and diabetes [2]. While both typical and atypical antipsychotics may effectively treat psychosis and other positive symptoms of schizophrenia, they are less effective at counteracting negative symptoms and, essentially, not effective regarding cognitive deficits. Thus, finding new pharmacotherapies for schizophrenia—which would be effective not only at positive symptoms but also at negative symptoms and cognitive deficits and would be devoid of significant side-effects—remains an important area of unmet need in the treatment of schizophrenia [3].

Over the last 60 years, there were many attempts to develop novel therapies for schizophrenia that exert antipsychotic action without blocking dopamine D₂ receptors; however, essentially, all these approaches failed in the clinical trials. Recently, a new promising molecular target for the treatment of schizophrenia—trace amine-associated receptor 1 (TAAR1)—has been identified. TAAR1 is a member of a relatively recently discovered family of mammalian G protein-coupled receptors called TAARs, which are activated by trace amines [4,5]. Biogenic trace amines are structurally and functionally related to classical monoaminergic neurotransmitters, such as dopamine and serotonin, but are present in much lower concentrations in the brain. In humans, six functional TAARs have been discovered [6]. The best-characterized member of the TAAR family is TAAR1 [6]. TAAR1 is widely expressed throughout the brain and has been found in areas that are associated with the emergence of schizophrenia symptoms, including the frontal cortex as well as the ventral tegmental area and dorsal raphe nucleus, which produce dopamine and serotonin, respectively. Moreover, preclinical studies indicate that TAAR1 can modulate the activity of several neurotransmitter systems (such as dopamine, serotonin, and glutamate), which dysregulation is believed to be involved in the pathogenesis of schizophrenia. Preclinical studies have shown that TAAR1 agonists produce antipsychotic-like effects in several animal models [7].

Currently, two substances with TAAR1 agonistic activity, Ulotaront (SEP-363856, SEP-856, Sunovion Pharmaceuticals Inc.) and Ralmitaront (RG-7906, RO-6889450, F. Hoffmann-La Roche AG), are undergoing clinical trials for the treatment of schizophrenia, schizoaffective disorder, and Parkinson's disease psychosis [6]. While the selective partial TAAR1 agonist Ralmitaront is currently being tested in Phase 2 clinical trials, Ulotaront (TAAR1 agonist with serotonin 5-HT_{1A} agonist activity) has entered Phase 3 clinical studies to evaluate the treatment of adults and adolescents with schizophrenia [8,9]. Results of Phase 2 studies with Ulotaront showed that this drug significantly reduced both positive and negative symptoms of schizophrenia, with a safety and tolerability profile comparable to placebo without significantly increasing weight, elevating prolactin or glucose, or inducing EPS. Based on such a promising therapeutic and safety profile in clinical trials, Ulotaront was awarded a Breakthrough Therapy designation by the US Food and Drug Administration (FDA). Since Ulotaront lacks an effect on dopamine D₂ receptors [8], it has emerged as the first antipsychotic compound effective clinically in schizophrenia without blocking D₂ dopamine receptors [9]. Additionally, the results of preclinical studies point to the possibility that TAAR1 agonists may have antianxiety [10], antidepressant [10,11], antiaddictive [12], and anticompulsive [13] effects.

Despite TAAR1 being the hot issue in psychopharmacology, a very limited number of potent and selective TAAR1 ligands are being investigated. Moreover, all preclinically used selective TAAR1 agonists chemically belong either to imidazole (e.g., RO5073012) [14] or to 2-aminooxazoline (e.g., RO5166017) [15] chemical classes (Figure 1). Although other chemical classes, such as biguanides derivatives [16], have been identified as TAAR1 agonists, screening of those compounds has been limited to *in silico* and *in vitro* analysis. The present study was aimed at (1) identifying novel TAAR1 agonists, chemically distinct from known chemical classes, and (2) testing the compounds found to be active at the TAAR1 receptor for their effects *in vivo* using animal models relevant to schizophrenia.

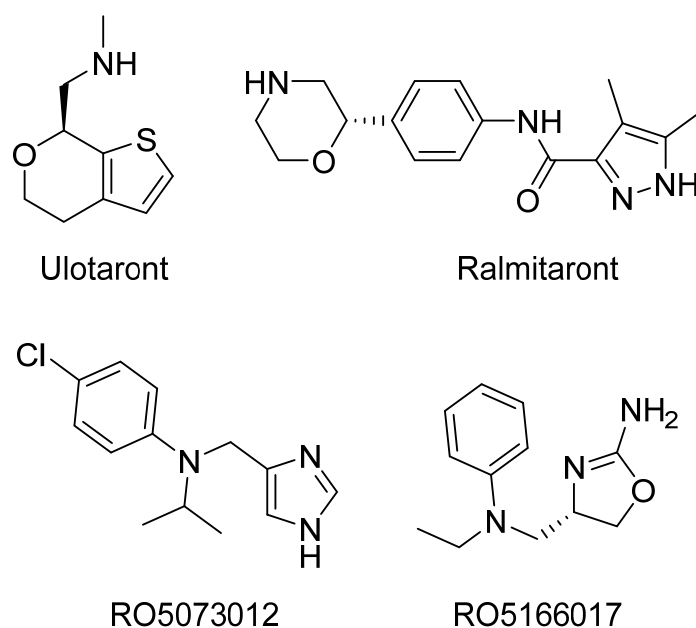


Figure 1. Advanced TAAR1 agonists at various stages of investigation: Ulotaront (phase III clinical trials), Ralmitaront (phase II clinical trials), RO5073012 (preclinical investigation), and RO5166017 (preclinical investigation).

2. Materials and Methods

2.1. General Experimental Procedures

All reactions were conducted in oven-dried glassware in an atmosphere of nitrogen. Melting points were measured with a Buchi B-520 melting point apparatus and were not corrected. Analytical thin-layer chromatography was carried out on Silufol UV-254 silica gel plates using appropriate mixtures of ethyl acetate and hexane. Compounds were visualized with short-wavelength UV light. The ^1H nuclear magnetic resonance (NMR) and ^{13}C NMR spectra (see Supporting Information) were recorded on Bruker MSL-300 spectrometers in dimethyl sulfoxide (DMSO)- d_6 or CDCl_3 using tetramethylsilane as an internal standard. Mass spectra were recorded using a Shimadzu LCMS-2020 system with ESI. All reagents and solvents were obtained from commercial sources and used without purification.

2.2. General Procedure 1—Synthesis of Compounds 6–57

Compound 4 (1.2 equiv.) was dissolved in dry methanol (5 mL/mmol) and treated with acyl hydrazide 3 (1.0 equiv.). The reaction mixture was stirred at room temperature for 24–48 h while the progress of the reaction was monitored by TLC analysis (2% MeOH in chloroform). The volatiles were removed on a rotary evaporator and the residue was transferred into a flask equipped with a Vigreux column and melted neat at 180–200 °C for 1–2 h. On cooling, the residue was purified by column chromatography on silica gel using 2% MeOH in chloroform as an eluent. Fractions containing the triazole product were pooled, concentrated in vacuo, and the residue was treated with 4M solution of HCl in 1,4-dioxane (1 h, room temperature). Following concentration on a rotary evaporator, the crystalline residue was triturated with ether, the solids were filtered off, washed with more ether, and air-dried to provide an analytically pure title compound as crystalline residue.

2.2.1. 2-(5-(4-Methoxyphenyl)-4H-1,2,4-triazol-3-yl)ethan-1-amine Hydrochloride (6)

Yield 0.21 g (60%). M.p. 248–250 °C. ^1H NMR (300 MHz, DMSO- d_6) δ 8.28 (s, 3H), 8.12 (d, J = 8.5 Hz, 2H), 7.12 (d, J = 8.6 Hz, 2H), 3.83 (s, 3H), 3.35–3.26 (m, 2H), 3.24–3.17 (m, 2H). ^{13}C NMR (75 MHz, DMSO- d_6) δ 161.5, 154.8, 154.5, 128.5, 118.0, 114.6, 55.5, 36.6, 24.1. HRMS (ESI) calcd for $\text{C}_{11}\text{H}_{15}\text{N}_4\text{O}$ [$\text{M} + \text{H}^+$] 219.1240 Da, found 219.1240 Da.

2.2.2. 2-(5-(3-Methoxyphenyl)-4H-1,2,4-triazol-3-yl)ethan-1-amine Hydrochloride (7)

Yield 0.92 g (48%). M.p. 235–236 °C. ¹H NMR (300 MHz, DMSO-*d*₆) δ 8.27 (br.s, 3H), 7.71–7.66 (m, 2H), 7.44 (t, J = 8.0 Hz, 1H), 7.11–7.05 (m, 1H), 3.82 (s, 3H), 3.33–3.24 (m, 2H), 3.22–3.14 (m, 2H). ¹³C NMR (75 MHz, DMSO-*d*₆) δ 159.6, 156.1, 155.6, 130.2, 128.7, 118.6, 116.3, 111.4, 55.4, 36.8, 24.3. HRMS (ESI) calcd for C₁₁H₁₅N₄O [M + H⁺] 219.1240 Da, found 219.1240 Da

2.2.3. 2-(5-(3-[Trifluoromethyl]phenyl)-4H-1,2,4-triazol-3-yl)ethan-1-amine Hydrochloride (8)

Yield 0.11 g (22%). M.p. 242–244 °C. ¹H NMR (300 MHz, DMSO-*d*₆) δ 8.35 (br.s, 5H), 7.89–7.67 (m, 2H), 3.35–3.14 (m, 4H). ¹³C NMR (75 MHz, DMSO-*d*₆) δ 156.9, 155.6, 130.4, 130.3, 130.0 (q, J = 31.8 Hz), 129.9, 126.2 (q, J = 3.5 Hz), 124.1 (q, J = 272.4 Hz), 122.4 (q, J = 3.8 Hz), 36.8, 24.2. HRMS (ESI) calcd for C₁₁H₁₁F₃N₄ [M + H⁺] 257.1009 Da, found 1009 Da.

2.2.4. 2-(5-(4-[Trifluoromethoxy]phenyl)-4H-1,2,4-triazol-3-yl)ethan-1-amine Hydrochloride (9)

Yield 0.054 g (12%). M.p. 253–254 °C. ¹H NMR (300 MHz, DMSO-*d*₆) δ 8.28 (br.s, 3H), 8.20–8.14 (m, 2H), 7.53–7.47 (m, 2H), 3.30–3.21 (m, 2H), 3.20–3.12 (m, 2H). ¹³C NMR (75 MHz, DMSO-*d*₆) δ 157.1, 155.9, 149.1 (q, J = 1.6 Hz), 128.6, 128.1, 121.5, 118.4 (q, J = 256.7 Hz), 36.9, 24.4. HRMS (ESI) calcd for C₁₁H₁₁F₃N₄O [M + H⁺] 273.0958 Da, found 273.0958 Da.

2.2.5. 2-(5-(Pyridin-4-yl)-4H-1,2,4-triazol-3-yl)ethan-1-amine Hydrochloride (10)

Yield 0.06 g (18%). M.p. 257–258 °C. ¹H NMR (300 MHz, DMSO-*d*₆) δ 8.95 (d, J = 6.6 Hz, 2H), 8.46 (d, J = 6.6 Hz, 2H), 8.31 (s, 1H), 3.34–3.18 (m, 4H). ¹³C NMR (75 MHz, DMSO-*d*₆) δ 156.68, 156.08, 151.10, 145.15, 143.38, 124.02, 122.41, 36.63, 23.99. HRMS (ESI) calcd for C₉H₁₁N [M + H⁺] 190.1087 Da, found 190.1087 Da.

2.2.6. 2-(5-(3,4-Dimethoxyphenyl)-4H-1,2,4-triazol-3-yl)ethan-1-amine Hydrochloride (11)

Yield 0.45 g (26%). M.p. 209–210 °C. ¹H NMR (300 MHz, DMSO-*d*₆) δ 8.07 (br.s, 3H), 7.6–7.59 (m, 2H), 7.1–7.07 (m, 1H), 3.84 (s, 3H), 3.81 (s, 3H), 3.29–3.17 (m, 2H), 3.13–3.03 (m, 2H). ¹³C NMR (75 MHz, DMSO-*d*₆) δ 154.9, 154.6, 150.9, 148.8, 119.7, 117.7, 111.8, 109.7, 55.7, 55.5, 36.5, 24.0. HRMS (ESI) calcd for C₁₂H₁₇N₄O₂ [M + H⁺] 249.1346 Da, found 249.1346 Da.

2.2.7. 2-(5-(4-Bromo-3-methylphenyl)-4H-1,2,4-triazol-3-yl)ethan-1-amine Hydrochloride (12)

Yield 0.139 g (36%). M.p. 251–252 °C. ¹H NMR (300 MHz, DMSO-*d*₆) δ 8.18 (br.s, 3H), 8.03–8.00 (m, 1H), 7.80–7.75 (m, 1H), 7.72–7.68 (m, 1H), 3.30–3.18 (m, 2H), 3.17–3.08 (m, 2H), 2.41 (s, 3H). ¹³C NMR (75 MHz, DMSO-*d*₆) δ 156.9, 155.8, 138.2, 132.9, 128.6, 128.2, 125.8, 125.5, 37.0, 24.4, 22.6. HRMS (ESI) calcd for C₁₁H₁₄BrN₄ [M + H⁺] 281.0396 Da, found 281.0396 Da.

2.2.8. 2-(5-(Diphenylmethyl)-4H-1,2,4-triazol-3-yl)ethan-1-amine Hydrochloride (13)

Yield 0.15 g (42%). M.p. 236–237 °C. ¹H NMR (300 MHz, DMSO-*d*₆) δ 8.16 (br.s, 3H), 7.39–7.19 (m, 10H), 5.65 (s, 1H), 3.24–3.13 (m, 2H), 3.10–3.03 (m, 2H). ¹³C NMR (75 MHz, DMSO-*d*₆) δ 158.9, 154.6, 140.4, 128.4, 128.4, 126.8, 48.2, 36.3, 23.9. HRMS (ESI) calcd for C₁₇H₁₉N₄ [M + H⁺] 279.1604 Da, found 279.1604 Da.

2.2.9. 2-(5-(4-Nitrophenyl)-4H-1,2,4-triazol-3-yl)ethan-1-amine Hydrochloride (14)

Yield 1.959 g (40%). M.p. 239–240 °C. ¹H NMR (300 MHz, DMSO-*d*₆) δ 8.39–8.25 (m, 4H), 8.20 (br.s, 3H), 3.31–3.21 (m, 2H), 3.19–3.11 (m, 2H). ¹³C NMR (75 MHz, DMSO-*d*₆) δ 158.0, 155.9, 147.0, 136.4, 127.1, 124.4, 37.0, 24.3. HRMS (ESI) calcd for C₁₀H₁₂N₅O₂ [M + H⁺] 234.0986 Da, found 234.0986 Da.

2.2.10. 2-(5-(4-[Trifluoromethyl]phenyl)-4*H*-1,2,4-triazol-3-yl)ethan-1-amine Hydrochloride (**15**)

Yield 0.629 g (46%). M.p. 254–255 °C. ¹H NMR (300 MHz, DMSO-*d*₆) δ 8.28–8.19 (m, 5H), 7.8–7.82 (m, 2H), 3.33–3.21 (m, 2H), 3.19–3.11 (m, 2H). ¹³C NMR (75 MHz, DMSO-*d*₆) δ 157.8, 155.9, 133.8, 129.4 (q, J = 31.9 Hz), 126.6, 125.9 (q, J = 3.7 Hz), 124.2 (q, J = 272.1 Hz), 37.0, 24.4. HRMS (ESI) calcd for C₁₁H₁₂F₃N₄ [M + H⁺] 257.1009 Da, found 257.1009 Da.

2.2.11. 2-(5-(Thiophen-2-yl)-4*H*-1,2,4-triazol-3-yl)ethan-1-amine Hydrochloride (**16**)

Yield 0.164 g (24%). M.p. 248–250 °C. ¹H NMR (300 MHz, DMSO-*d*₆) δ 8.17 (br.s, 3H), 7.71–7.62 (m, 2H), 7.19–7.14 (m, 1H), 3.27–3.15 (m, 2H), 3.13–3.04 (m, 2H). ¹³C NMR (75 MHz, DMSO-*d*₆) δ 155.1, 153.3, 130.8, 127.6, 127.3, 126.1, 36.3, 23.7. HRMS (ESI) calcd for C₈H₁₁N₄S [M + H⁺] 195.0699 Da, found 195.0699 Da.

2.2.12. 2-(5-(Phenoxymethyl)-4*H*-1,2,4-triazol-3-yl)ethan-1-amine Hydrochloride (**17**)

Yield 0.283 g (14%). M.p. 206–207 °C. ¹H NMR (300 MHz, DMSO-*d*₆) δ 8.26 (br.s, 3H), 7.34–7.27 (m, 2H), 7.07–7.01 (m, 2H), 7.00–6.93 (m, 1H), 5.12 (s, 2H), 3.24–3.15 (m, 2H), 3.14–3.08 (m, 2H). ¹³C NMR (75 MHz, DMSO-*d*₆) δ 157.7, 155.6, 155.3, 129.4, 121.0, 114.5, 61.6, 36.6, 24.1. HRMS (ESI) calcd for C₁₁H₁₅N₄O [M + H⁺] 219.1240 Da, found 219.1240 Da.

2.2.13. 2-(5-(3-[Trifluoromethyl]phenyl)-4*H*-1,2,4-triazol-3-yl)ethan-1-amine Hydrochloride (**18**)

Yield 1.25 g (60%). M.p. 288–290 °C. ¹H NMR (300 MHz, DMSO-*d*₆) δ 8.37–8.33 (m, 1H), 8.23 (br.s, 3H), 7.77–7.73 (m, 2H), 3.32–3.22 (m, 2H), 3.20–3.12 (m, 2H). ¹³C NMR (75 MHz, DMSO-*d*₆) δ 155.1, 151.9, 128.3, 128.1, 126.8, 125.9, 36.7, 24.2. HRMS (ESI) calcd for C₈H₁₁N₄S [M + H⁺] 195.0699 Da, found 195.0699 Da.

2.2.14. 2-(5-(4-(Benzyloxy)phenyl)-4*H*-1,2,4-triazol-3-yl)ethan-1-amine Hydrochloride (**19**)

Yield 4.568g (54%). M.p. 238–240 °C. ¹H NMR (300 MHz, DMSO-*d*₆) δ 8.24 (br.s, 3H), 8.10–8.05 (m, 2H), 7.50–7.31 (m, 5H), 7.22–7.17 (m, 2H), 5.19 (s, 2H), 3.33–3.22 (m, 2H), 3.20–3.13 (m, 1H). ¹³C NMR (75 MHz, DMSO-*d*₆) δ 160.0, 155.3, 155.0, 136.4, 128.2, 128.0, 127.8, 127.7, 118.9, 115.2, 69.3, 36.6, 24.1. HRMS (ESI) calcd for C₁₇H₁₉N₄O [M + H⁺] 295.1553Da, found 295.1553 Da.

2.2.15. 2-(5-(3-Bromophenyl)-4*H*-1,2,4-triazol-3-yl)ethan-1-amine Hydrochloride (**20**)

Yield 4.06 g (45%). M.p. 239–241 °C. ¹H NMR (300 MHz, DMSO-*d*₆) δ 8.33 (br.s, 3H), 8.24 (s, 1H), 8.07 (d, J = 7.8 Hz, 1H), 7.69–7.64 (m, 1H), 7.51–7.44 (m, 1H), 3.32–3.22 (m, 2H), 3.21–3.14 (m, 2H). ¹³C NMR (75 MHz, DMSO-*d*₆) δ 156.4, 155.6, 132.5, 131.2, 131.1, 128.6, 125.1, 122.2, 36.8, 24.2. HRMS (ESI) calcd for C₁₀H₁₂BrN₄ [M + H⁺] 267.0239 Da, found 267.0239 Da.

2.2.16. 2-(5-(3,5-Dichlorophenyl)-4*H*-1,2,4-triazol-3-yl)ethan-1-amine Hydrochloride (**21**)

Yield 0.102 g (36%). M.p. 222–224 °C. ¹H NMR (300 MHz, DMSO-*d*₆) δ 8.31 (br.s, 3H), 8.02 (d, J = 1.8 Hz, 2H), 7.70–7.68 (m, 1H), 3.29–3.20 (m, 2H), 3.19–3.11 (m, 2H). ¹³C NMR (75 MHz, DMSO-*d*₆) δ 156.6, 155.8, 134.7, 133.3, 128.7, 124.3, 36.8, 24.1. HRMS (ESI) calcd for C₁₀H₁₁Cl₂N₄ [M + H⁺] 257.0355 Da, found 257.0355 Da.

2.2.17. 2-(5-Phenyl-4*H*-1,2,4-triazol-3-yl)ethan-1-amine Hydrochloride (**22**)

Yield 0.04 g (8%). M.p. 250–252 °C. ¹H NMR (300 MHz, DMSO-*d*₆) δ 8.17 (br.s, 3H), 8.08–8.02 (m, 2H), 7.55–7.44 (m, 3H), 3.32–3.20 (m, 2H), 3.17–3.09 (m, 2H). ¹³C NMR (75 MHz, DMSO-*d*₆) δ 156.6, 154.1, 129.9, 129.0, 128.5, 126.1, 37.2, 24.6. HRMS (ESI) calcd for C₁₀H₁₃N₄ [M + H⁺] 189.1135 Da, found 189.1135 Da.

2.2.18. 2-(5-(2-Methylphenyl)-4H-1,2,4-triazol-3-yl)ethan-1-amine Hydrochloride (24)

Yield 0.110 g (22%). M.p. 235–236 °C. ¹H NMR (300 MHz, DMSO-*d*₆) δ 8.25 (br.s, 3H), 7.78 (d, J = 7.4 Hz, 1H), 7.43–7.29 (m, 3H), 3.33–3.22 (m, 2H), 3.21–3.14 (m, 2H), 2.53 (s, 3H). ¹³C NMR (75 MHz, DMSO-*d*₆) δ 157.1, 155.1, 136.6, 131.1, 129.0, 129.2, 127.5, 125.9, 36.8, 30.6, 24.3. HRMS (ESI) calcd for C₁₁H₁₅N₄ [M + H⁺] 203.1291 Da, found 203.1291 Da.

2.2.19. 3-(5-(2-Aminoethyl)-4H-1,2,4-triazol-3-yl)-N,N-dimethylaniline Hydrochloride (8)

Yield 0.022 g (22%). M.p. 179–181 °C. ¹H NMR (300 MHz, DMSO-*d*₆) δ 8.42 (br.s, 3H), 8.28 (s, 1H), 7.97 (d, J = 6.9 Hz, 1H), 7.67–7.56 (m, 2H), 3.38–3.21 (m, 4H), 3.12 (s, 6H). ¹³C NMR (75 MHz, DMSO-*d*₆) δ 156.0, 154.8, 146.0, 130.8, 128.8, 123.4, 120.6, 116.6, 44.2, 36.7, 24.1. HRMS (ESI) calcd for C₁₂H₁₈N₅ [M + H⁺] 232.1557 Da, found 232.1557 Da.

2.2.20. 2-(5-(4-Ethoxyphenyl)-4H-1,2,4-triazol-3-yl)ethan-1-amine Hydrochloride (26)

Yield 0.051 g (44%). M.p. 235–236 °C. ¹H NMR (300 MHz, DMSO-*d*₆) δ 8.16 (br.s, 3H), 8.01 (d, J = 8.7 Hz, 2H), 7.06 (d, J = 8.8 Hz, 2H), 4.10 (q, J = 6.9 Hz, 2H), 3.31–3.19 (m, 2H), 3.17–3.08 (m, 2H), 1.34 (t, J = 6.9 Hz, 3H). ¹³C NMR (75 MHz, DMSO-*d*₆) δ 160.3, 156.8, 156.4, 128.1, 120.1, 115.1, 63.6, 37.3, 24.9, 14.8. HRMS (ESI) calcd for C₁₂H₁₇N₄O [M + H⁺] 233.1397 Da, found 233.1397 Da.

2.2.21. 2-(5-(4-Ethylphenyl)-4H-1,2,4-triazol-3-yl)ethan-1-amine Hydrochloride (27)

Yield 0.01 g (5%). M.p. 119–121 °C. ¹H NMR (300 MHz, DMSO-*d*₆) δ 8.21 (s, 3H), 7.99 (d, J = 6.8 Hz, 2H), 7.36 (d, J = 6.6 Hz, 2H), 3.35–3.21 (m, 2H), 3.19–3.09 (m, 2H), 2.66 (q, J = 6.7 Hz, 2H), 1.21 (s, J = 6.7 Hz, 3H). ¹³C NMR (75 MHz, DMSO-*d*₆) 156.3, 155.8, 146.3, 128.4, 126.4, 124.9, 36.9, 28.1, 24.5, 15.3. HRMS (ESI) calcd for C₁₂H₁₇N₄ [M + H⁺] 217.1447 Da, found 217.1447 Da.

2.2.22. 2-(5-(2-Nitrophenyl)-4H-1,2,4-triazol-3-yl)ethan-1-amine Hydrochloride (27)

Yield 0.111 g (94%). M.p. 169–170 °C. ¹H NMR (300 MHz, DMSO-*d*₆) δ 8.36–8.23 (m, 6H), 3.33–3.13 (m, 4H). ¹³C NMR (75 MHz, DMSO-*d*₆) δ 156.0, 154.8, 148.8, 132.1, 130.4, 130.1, 123.6, 123.3, 36.7, 24.0. HRMS (ESI) calcd for C₁₀H₁₂N₅O₂ [M + H⁺] 234.0986 Da, found 234.0986 Da.

2.2.23. 2-(5-(4-Chlorophenyl)-4H-1,2,4-triazol-3-yl)ethan-1-amine Hydrochloride (28)

Yield 0.025 g (13%). M.p. 239–241 °C. ¹H NMR (300 MHz, DMSO-*d*₆) δ 8.12 (s, 2H), 8.05–8.00 (m, 2H), 7.58–7.53 (m, 2H), 3.29–3.17 (m, 2H), 3.14–3.05 (m, 2H). ¹³C NMR (75 MHz, DMSO-*d*₆) δ 157.7, 156.4, 134.3, 129.2, 128.3, 127.9, 37.2, 24.6. HRMS (ESI) calcd for C₁₀H₁₂ClN₄ [M + H⁺] 223.0745 Da, found 223.0745 Da.

2.2.24. 2-(5-(2-Bromophenyl)-4H-1,2,4-triazol-3-yl)ethan-1-amine Hydrochloride (29)

Yield 0.044 g (33%). M.p. 194–196 °C. ¹H NMR (300 MHz, DMSO-*d*₆) δ 8.25 (s, 3H), 7.79–7.73 (m, 2H), 7.53–7.46 (m, 1H), 7.44–7.38 (m, 1H), 3.29–3.11 (m, 4H). ¹³C NMR (75 MHz, DMSO-*d*₆) δ 157.4, 155.8, 133.8, 131.9, 131.4, 131.0, 128.0, 121.3, 37.2, 24.6. HRMS (ESI) calcd for C₁₀H₁₂BrN₄ [M + H⁺] 267.0240 Da, found 267.0240 Da.

2.2.25. 4-(5-(2-Aminoethyl)-4H-1,2,4-triazol-3-yl)-N,N-dimethylaniline (30)

Yield 0.017 g (9%). M.p. 244–246 °C. ¹H NMR (300 MHz, DMSO-*d*₆) δ 8.20 (s, 3H), 8.02 (d, J = 8.7 Hz, 2H), 6.91 (d, J = 8.1 Hz, 2H), 3.35–3.24 (m, 2H), 3.21–3.12 (m, 2H), 3.03 (s, 6H). ¹³C NMR (75 MHz, DMSO-*d*₆) δ 154.2, 154.1, 151.8, 128.2, 112.3, 36.6, 25.5, 24.1. HRMS (ESI) calcd for C₁₂H₁₈N [M + H⁺] 232.1557 Da, found 232.1557 Da.

2.2.26. 2-(5-(3,5-Dimethylphenyl)-4H-1,2,4-triazol-3-yl)ethan-1-amine Hydrochloride (31)

Yield 0.138 g (41%). M.p. 232–234 °C. ¹H NMR (300 MHz, DMSO-*d*₆) δ 8.34 (br.s, 3H), 7.76 (s, 2H), 7.17 (s, 1H), 3.37–3.16 (m, 4H), 2.33 (s, 6H). ¹³C NMR (75 MHz, DMSO-*d*₆) δ

155.7, 155.2, 138.4, 132.2, 126.5, 124.3, 36.7, 24.2, 21.0. HRMS (ESI) calcd for $C_{12}H_{17}N_4$ [$M + H^+$] 217.1448 Da, found 217.1448 Da.

2.2.27. 2-(5-(3,4,5-Triethoxyphenyl)-4*H*-1,2,4-triazol-3-yl)ethan-1-amine Hydrochloride (32)

Yield 0.071 g (26%). M.p. 253–255 °C. 1H NMR (300 MHz, DMSO- d_6) δ 8.22 (br.s, 3H), 7.48 (s, 2H), 4.11 (q, $J = 6.8$ Hz, 4H), 4.00 (q, $J = 7.0$ Hz, 2H), 3.34–3.23 (m, 2H), 3.21–3.12 (m, 2H), 1.36 (t, $J = 6.9$ Hz, 6H), 1.24 (t, $J = 7.0$ Hz, 3H). ^{13}C NMR (75 MHz, DMSO- d_6) δ 156.0, 155.9, 152.8, 138.7, 122.0, 104.8, 68.1, 64.3, 36.9, 24.5, 15.5, 14.8. HRMS (ESI) calcd for $C_{16}H_{25}N_4O_3$ [$M + H^+$] 321.1921 Da, found 321.1921 Da.

2.2.28. 2-(5-(3,5-Dimethoxyphenyl)-4*H*-1,2,4-triazol-3-yl)ethan-1-amine Hydrochloride (33)

Yield 0.031 g (15%). M.p. 245–247 °C. 1H NMR (300 MHz, DMSO- d_6) δ 8.10 (br.s, 3H), 7.20 (d, $J = 2.2$ Hz, 2H), 6.59 (t, $J = 2.1$ Hz, 1H), 3.80 (s, 6H), 3.29–3.17 (m, 2H), 3.12–3.04 (m, 2H). ^{13}C NMR (75 MHz, DMSO- d_6) δ 160.8, 157.2, 154.1, 125.2, 143.0, 101.8, 55.5, 37.1, 24.7. HRMS (ESI) calcd for $C_{12}H_{17}N_4O$ [$M + H^+$] 249.1346 Da, found 249.1346 Da.

2.2.29. 2-(5-(4-Fluorophenyl)-4*H*-1,2,4-triazol-3-yl)ethan-1-amine Hydrochloride (34)

Yield 0.028 g (16%). M.p. 253–256 °C. 1H NMR (300 MHz, DMSO- d_6) δ 8.25–8.04 (m, 5H), 7.46–7.27 (m, 2H), 3.30–3.19 (m, 2H), 3.17–3.08 (m, 2H). ^{13}C NMR (75 MHz, DMSO- d_6) δ 162.93 (d, $J = 246.5$ Hz), 156.89, 155.93, 128.38 (d, $J = 8.7$ Hz), 125.56, 115.97 (d, $J = 22.0$ Hz), 36.94, 24.45. HRMS (ESI) calcd for $C_{10}H_{12}FN_4$ [$M + H^+$] 207.1041 Da, found 207.1041 Da.

2.2.30. 2-(5-(Quinolin-6-yl)-4*H*-1,2,4-triazol-3-yl)ethan-1-amine Hydrochloride (35)

Yield 0.037 g (18%). M.p. 265–267 °C. 1H NMR (300 MHz, DMSO- d_6) δ 9.20 (d, $J = 4.8$ Hz, 1H), 9.05 (d, $J = 7.6$ Hz, 1H), 8.89 (s, 1H), 8.64 (d, $J = 8.9$ Hz, 1H), 8.38 (d, $J = 8.8$ Hz, 1H), 8.22 (br.s, 3H), 8.00–7.92 (m, 1H), 3.34–3.23 (m, 2H), 3.22–3.15 (m, 2H). ^{13}C NMR (75 MHz, DMSO- d_6) δ 158.4, 155.8, 146.6, 144.7, 140.1, 131.0, 130.6, 128.7, 125.6, 123.4, 122.7, 37.0, 24.3. HRMS (ESI) calcd for $C_{13}H_{14}N_5$ [$M + H^+$] 240.1244 Da, found 240.1244 Da.

2.2.31. 2-(5-(3-Nitrophenyl)-4*H*-1,2,4-triazol-3-yl)ethan-1-amine Hydrochloride (36)

Yield 0.057 g (48%). M.p. 214–216 °C. 1H NMR (300 MHz, DMSO- d_6) δ 8.78–8.76 (m, 1H), 8.44 (d, $J = 7.8$ Hz, 1H), 8.28 (dd, $J = 8.2, 1.6$ Hz, 1H), 8.18 (br.s, 3H), 7.79 (t, $J = 8.0$ Hz, 1H), 3.32–3.20 (m, 2H), 3.19–3.11 (m, 2H). ^{13}C NMR (75 MHz, DMSO- d_6) δ 157.9, 156.1, 148.5, 132.2, 132.0, 131.0, 124.2, 120.5, 37.2, 24.5. HRMS (ESI) calcd for $C_{10}H_{12}N_5O_2$ [$M + H^+$] 234.0986 Da, found 234.0986 Da.

2.2.32. 2-(5-(3,4-Dimethylphenyl)-4*H*-1,2,4-triazol-3-yl)ethan-1-amine Hydrochloride (37)

Yield 0.015 g (8%). M.p. 231–234 °C. 1H NMR (300 MHz, DMSO- d_6) δ 8.14 (br.s, 3H), 7.84 (s, 1H), 7.79–7.73 (m, 1H), 7.27 (d, $J = 7.8$ Hz, 1H), 3.30–3.18 (m, 2H), 3.14–3.06 (m, 2H), 2.28 (s, 3H), 2.27 (s, 3H). ^{13}C NMR (75 MHz, DMSO- d_6) δ 156.3, 153.5, 138.7, 136.9, 135.1, 130.0, 127.2, 123.7, 37.0, 24.6, 19.5, 19.4. HRMS (ESI) calcd for $C_{12}H_{17}N_4$ [$M + H^+$] 217.1448 Da, found 217.1448 Da.

2.2.33. 2-(5-(Pyrazin-2-yl)-4*H*-1,2,4-triazol-3-yl)ethan-1-amine Hydrochloride (38)

Yield 0.020 g (21%). M.p. 184–186 °C. 1H NMR (300 MHz, DMSO- d_6) δ 9.29 (d, $J = 1.3$ Hz, 1H), 8.77–8.72 (m, 2H), 8.16 (br.s, 3H), 3.29–3.20 (m, 2H), 3.17–3.10 (m, 2H). ^{13}C NMR (75 MHz, DMSO- d_6) δ 157.8, 155.4, 145.5, 144.7, 143.6, 142.7, 37.3, 24.9. HRMS (ESI) calcd for $C_8H_{11}N_6$ [$M + H^+$] 191.1040 Da, found 191.1040 Da.

2.2.34. 2-(5-(2-[Trifluoromethoxy]phenyl)-4*H*-1,2,4-triazol-3-yl)ethan-1-amine Hydrochloride (39)

Yield 0.053 g (39%). M.p. 208–211 °C. 1H NMR (300 MHz, DMSO- d_6) δ 8.17–8.05 (m, 3H), 7.62–7.47 (m, 3H), 3.29–3.18 (m, 2H), 3.15–3.08 (m, 2H). ^{13}C NMR (75 MHz, DMSO- d_6) δ 155.18, 152.20, 145.18 (q, $J = 1.7$ Hz), 130.83, 130.47, 127.65, 123.78, 122.00, 119.96 (q,

$J = 256.5$ Hz), 36.80, 24.11. HRMS (ESI) calcd for $C_{11}H_{12}F_3N_4O$ $[M + H^+]$ 273.0957 Da, found 273.0957 Da.

2.2.35. 2-(5-(4-Butoxyphenyl)-4*H*-1,2,4-triazol-3-yl)ethan-1-amine Hydrochloride (**40**)

Yield 0.019 g (15%). M.p. 205–207 °C. 1H NMR (300 MHz, DMSO- d_6) δ 8.32 (br.s, 3H), 8.06 (d, $J = 8.7$ Hz, 2H), 7.08 (d, $J = 8.8$ Hz, 2H), 4.04 (t, $J = 6.4$ Hz, 2H), 3.33–3.12 (m, 4H), 1.76–1.65 (m, 2H), 1.50–1.37 (m, 2H), 0.93 (t, $J = 7.4$ Hz, 3H). ^{13}C NMR (75 MHz, DMSO- d_6) δ 160.4, 155.7, 155.6, 128.1, 119.2, 114.9, 67.4, 36.8, 30.6, 24.4, 18.7, 13.7. HRMS (ESI) calcd for $C_{14}H_{21}N_4O$ $[M + H^+]$ 261.1709 Da, found 261.1709 Da.

2.2.36. 2-(5-(3-Iodophenyl)-4*H*-1,2,4-triazol-3-yl)ethan-1-amine Hydrochloride (**41**)

Yield 0.053 g (39%). M.p. 224–225 °C. 1H NMR (300 MHz, DMSO- d_6) δ 8.37 (t, $J = 1.6$ Hz, 1H), 8.17 (br.s, 3H), 8.06–8.01 (m, 1H), 7.83–7.78 (m, 1H), 7.29 (t, $J = 7.8$ Hz, 1H), 3.28–3.17 (m, 2H), 3.15–3.07 (m, 2H). ^{13}C NMR (75 MHz, DMSO- d_6) δ 157.3, 156.6, 138.4, 134.5, 131.8, 131.4, 125.5, 95.4, 37.3, 24.7. HRMS (ESI) calcd for $C_{10}H_{12}IN_4$ $[M + H^+]$ 315.0101 Da, found 315.0101 Da.

2.2.37. 2-(5-(4-Iodo-3-methylphenyl)-4*H*-1,2,4-triazol-3-yl)ethan-1-amine Hydrochloride (**42**)

Yield 0.047 g (31%). M.p. 225–227 °C. 1H NMR (300 MHz, DMSO- d_6) δ 8.21 (br.s, 3H), 8.00 (d, $J = 1.8$ Hz, 1H), 7.94 (d, $J = 8.2$ Hz, 1H), 7.59 (dd, $J = 8.2, 2.0$ Hz, 1H), 3.30–3.18 (m, 2H), 3.16–3.08 (m, 2H), 2.43 (s, 3H). ^{13}C NMR (75 MHz, DMSO- d_6) δ 157.5, 156.3, 141.6, 139.3, 129.5, 127.2, 125.3, 102.9, 37.1, 27.7, 24.6. HRMS (ESI) calcd for $C_{11}H_{14}IN_4$ $[M + H^+]$ 329.0257 Da, found 329.0257 Da.

2.2.38. 2-(5-(4-[(2-Fluorobenzyl)oxy]phenyl)-4*H*-1,2,4-triazol-3-yl)ethan-1-amine Hydrochloride (**43**)

Yield 0.023 g (15%). M.p. 232–235 °C. 1H NMR (300 MHz, DMSO- d_6) δ 8.16 (br.s, 3H), 8.06–8.00 (m, 2H), 7.59 (t, $J = 7.0$ Hz, 1H), 7.49–7.40 (m, 1H), 7.32–7.17 (m, 4H), 5.22 (s, 2H), 3.31–3.19 (m, 2H), 3.17–3.08 (m, 2H). ^{13}C NMR (75 MHz, DMSO- d_6) δ 160.5 (d, $J = 246.2$ Hz), 159.5, 156.6, 156.4, 130.9 (d, $J = 4.0$ Hz), 130.6 (d, $J = 8.2$ Hz), 127.8, 124.6 (d, $J = 3.4$ Hz), 123.4 (d, $J = 14.5$ Hz), 120.8, 115.5 (d, $J = 21.0$ Hz), 115.1, 63.8, 37.1, 24.7. HRMS (ESI) calcd for $C_{17}H_{18}FN_4O$ $[M + H^+]$ 313.1459 Da, found 313.1459 Da.

2.2.39. 2-(5-(4-[(3-Fluorobenzyl)oxy]phenyl)-4*H*-1,2,4-triazol-3-yl)ethan-1-amine Hydrochloride (**44**)

Yield 0.051 g (31%). M.p. 214–216 °C. 1H NMR (300 MHz, DMSO- d_6) δ 8.20 (br.s, 3H), 8.08–8.02 (m, 2H), 7.51–7.40 (m, 1H), 7.35–7.28 (m, 2H), 7.23–7.13 (m, 3H), 5.21 (s, 2H), 3.32–3.20 (m, 2H), 3.18–3.10 (m, 2H). ^{13}C NMR (75 MHz, DMSO- d_6) δ 162.7 (d, $J = 243.6$ Hz), 160.1, 156.8, 156.6, 140.1 (d, $J = 7.5$ Hz), 131.0 (d, $J = 8.3$ Hz), 128.3, 124.1 (d, $J = 1.6$ Hz), 120.9, 115.8, 115.2 (d, $J = 21.0$ Hz), 114.8 (d, $J = 21.7$ Hz), 69.0, 37.5, 25.0. HRMS (ESI) calcd for $C_{17}H_{18}FN_4O$ $[M + H^+]$ 313.1459 Da, found 313.1459 Da.

2.2.40. 2-(5-(4-[(4-Fluorobenzyl)oxy]phenyl)-4*H*-1,2,4-triazol-3-yl)ethan-1-amine Hydrochloride (**45**)

Yield 0.070 g (46%). M.p. 220–222 °C. 1H NMR (300 MHz, DMSO- d_6) δ 8.20 (s, 3H), 8.08–8.01 (m, 2H), 7.53 (dd, $J = 8.6, 5.6$ Hz, 2H), 7.28–7.15 (m, 4H), 5.17 (s, 2H), 3.32–3.20 (m, 2H), 3.18–3.09 (m, 2H). ^{13}C NMR (75 MHz, DMSO- d_6) δ 162.3 (d, $J = 243.8$ Hz), 160.4, 156.3, 156.2, 133.4 (d, $J = 3.0$ Hz), 130.6 (d, $J = 8.3$ Hz), 128.5, 120.3, 115.8 (d, $J = 21.4$ Hz), 115.8, 69.2, 37.3, 24.9. HRMS (ESI) calcd for $C_{17}H_{18}FN_4O$ $[M + H^+]$ 313.1459 Da, found 313.1459 Da.

2.2.41. 2-(5-(4-[(2-Fluorobenzyl)oxy]-3-methylphenyl)-4*H*-1,2,4-triazol-3-yl)ethan-1-amine Hydrochloride (**46**)

Yield 0.045 g (27%). M.p. 234–236 °C. 1H NMR (300 MHz, DMSO- d_6) δ 8.18 (br.s, 3H), 7.96–7.91 (m, 2H), 7.63–7.57 (m, 1H), 7.48–7.40 (m, 1H), 7.31–7.23 (m, 3H), 5.24 (s, 2H),

3.32–3.19 (m, 2H), 3.16–3.09 (m, 2H), 2.22 (s, 3H). ^{13}C NMR (75 MHz, DMSO- d_6) δ 160.4 (d, $J = 246.1$ Hz), 157.9, 156.2, 156.0, 130.5 (d, $J = 2.5$ Hz), 130.4, 128.6, 126.8, 125.6, 124.6 (d, $J = 3.4$ Hz), 123.8 (d, $J = 14.4$ Hz), 119.8, 115.5 (d, $J = 20.9$ Hz), 112.1, 63.9, 37.0, 24.6, 16.1. HRMS (ESI) calcd for $\text{C}_{18}\text{H}_{20}\text{FN}_4\text{O}$ [$\text{M} + \text{H}^+$] 327.1616 Da, found 327.1616 Da.

2.2.42. 2-(5-(4-[(3-Fluorobenzyl)oxy]-3-methylphenyl)-4H-1,2,4-triazol-3-yl)ethan-1-amine Hydrochloride (**47**)

Yield 0.053 g (32%). M.p. 215–216 °C. ^1H NMR (300 MHz, DMSO- d_6) δ 8.19 (br.s, 3H), 7.97–7.89 (m, 2H), 7.51–7.42 (m, 1H), 7.37–7.28 (m, 2H), 7.22–7.13 (m, 2H), 5.24 (s, 2H), 3.33–3.19 (m, 2H), 3.18–3.09 (m, 2H), 2.28 (s, 3H). ^{13}C NMR (75 MHz, DMSO- d_6) δ 163.2 (d, $J = 243.6$ Hz), 159.2, 156.1, 155.8, 140.8 (d, $J = 7.4$ Hz), 131.5 (d, $J = 8.3$ Hz), 129.8, 127.9, 126.9, 124.2 (d, $J = 2.7$ Hz), 119.1, 115.6 (d, $J = 20.9$ Hz), 114.9 (d, $J = 21.9$ Hz), 113.1, 69.5, 37.6, 25.1, 17.1. HRMS (ESI) calcd for $\text{C}_{18}\text{H}_{20}\text{FN}_4\text{O}$ [$\text{M} + \text{H}^+$] 327.1616 Da, found 327.1616 Da.

2.2.43. 2-(5-(4-[(4-Fluorobenzyl)oxy]-3-methylphenyl)-4H-1,2,4-triazol-3-yl)ethan-1-amine Hydrochloride (**48**)

Yield 0.020 g (12%). M.p. 182–183 °C. ^1H NMR (300 MHz, DMSO- d_6) δ 8.12 (br.s, 3H), 7.90–7.85 (m, 2H), 7.57–7.48 (m, 2H), 7.28–7.14 (m, 3H), 5.18 (s, 2H), 3.30–3.15 (m, 2H), 3.12–3.04 (m, 2H), 2.24 (s, 3H). ^{13}C NMR (75 MHz, DMSO- d_6) δ 161.6 (d, $J = 243.6$ Hz), 157.5, 156.7, 156.4, 133.1 (d, $J = 3.0$ Hz), 129.5 (d, $J = 8.3$ Hz), 128.2, 126.5, 125.1, 120.2, 115.1 (d, $J = 21.4$ Hz), 111.9, 68.5, 37.0, 24.6, 16.0. HRMS (ESI) calcd for $\text{C}_{18}\text{H}_{20}\text{FN}_4\text{O}$ [$\text{M} + \text{H}^+$] 327.1616 Da, found 327.1616 Da.

2.2.44. 2-(5-(3-Methyl-4-[(4-(trifluoromethyl)benzyl)oxy]phenyl)-4H-1,2,4-triazol-3-yl) Hydrochloride (**49**)

Yield 0.048 g (25%). M.p. 208–210 °C. ^1H NMR (300 MHz, DMSO- d_6) δ 8.18 (br.s, 3H), 7.95–7.88 (m, 2H), 7.82–7.67 (m, 4H), 7.17 (d, $J = 8.4$ Hz, 1H), 5.33 (s, 2H), 3.32–3.19 (m, 2H), 3.17–3.08 (m, 2H), 2.29 (s, 3H). ^{13}C NMR (75 MHz, DMSO- d_6) δ 158.0, 155.5, 155.3, 128.8, 128.4 (q, $J = 31.7$ Hz), 127.8, 127.8, 126.9, 125.8, 125.5 (q, $J = 3.8$ Hz), 124.3 (q, $J = 272.0$ Hz), 118.9, 112.1, 68.5, 36.8, 24.4, 16.2. HRMS (ESI) calcd for $\text{C}_{19}\text{H}_{20}\text{F}_3\text{N}_4\text{O}$ [$\text{M} + \text{H}^+$] 377.1584 Da, found 377.1584 Da.

2.2.45. 2-(5-(2-[3,4-Difluorophenoxy]phenyl)-4H-1,2,4-triazol-3-yl) Hydrochloride (**50**)

Yield 0.017 g (7%). M.p. 196–199 °C. ^1H NMR (300 MHz, DMSO- d_6) δ 8.22 (s, 3H), 8.10–8.04 (m, 1H), 7.54–7.43 (m, 1H), 7.36–7.19 (m, 2H), 7.04 (dt, $J = 5.9, 2.9$ Hz, 1H), 6.95–6.84 (m, 1H), 6.61–6.55 (m, 1H), 3.28–3.17 (m, 2H), 3.17–3.07 (m, 2H). ^{13}C NMR (75 MHz, DMSO- d_6) δ 157.30–152.35 (m), 154.79, 151.94 (d, $J = 1.7$ Hz), 150.19–146.62 (m), 132.17–130.40 (m), 124.52, 123.63, 118.00, 117.77, 116.91–115.14 (m), 111.52–108.80 (m), 106.72, 37.30, 25.06. HRMS (ESI) calcd for $\text{C}_{16}\text{H}_{15}\text{F}_2\text{N}_4\text{O}$ [$\text{M} + \text{H}^+$] 317.1208 Da, found 317.1208 Da.

2.2.46. 2-(5-(4-[3,4-Dimethylphenoxy]phenyl)-4H-1,2,4-triazol-3-yl)ethan-1-amine Hydrochloride (**51**)

Yield 0.01 g (5%). M.p. 201–203 °C. ^1H NMR (300 MHz, DMSO- d_6) δ 8.16 (s, 3H), 8.06–7.99 (m, 2H), 7.18 (d, $J = 8.1$ Hz, 1H), 7.09–7.02 (m, 2H), 6.91 (d, $J = 2.4$ Hz, 1H), 6.85–6.79 (m, 1H), 3.30–3.18 (m, 2H), 3.16–3.07 (m, 2H), 2.21 (s, 6H). ^{13}C NMR (75 MHz, DMSO- d_6) δ 158.5, 157.8, 156.6, 151.2, 134.2, 132.4, 131.0, 130.9, 129.5, 128.3, 120.5, 120.1, 118.0, 113.7, 37.4, 24.7, 20.6, 15.9. HRMS (ESI) calcd for $\text{C}_{18}\text{H}_{21}\text{N}_4\text{O}$ [$\text{M} + \text{H}^+$] 309.1710 Da, found 309.1710 Da.

2.2.47. 2-(5-(3-[2,4-Dimethylphenoxy]phenyl)-4H-1,2,4-triazol-3-yl)ethan-1-amine Hydrochloride Hydrochloride (**52**)

Yield 0.052 g (23%). M.p. 308–310 °C. ^1H NMR (300 MHz, DMSO- d_6) δ 8.19 (br.s, 3H), 7.76–7.66 (m, 1H), 7.52–7.35 (m, 2H), 7.15 (br.s, 1H), 7.09–7.00 (m, 1H), 6.98–6.83 (m, 2H), 3.26–3.04 (m, 4H), 2.28 (s, 3H), 2.10 (s, 3H). ^{13}C NMR (75 MHz, DMSO- d_6) δ 159.2, 157.1,

156.8, 153.7, 138.7, 132.6, 131.2, 128.2, 123.2, 120.9, 118.1, 117.1, 37.4, 24.9, 19.7, 18.9. HRMS (ESI) calcd for C₁₈H₂₁N₄O [M + H⁺] 309.1710 Da, found 309.1710 Da.

2.2.48. 2-(5-(3-[2-Chlorophenoxy]phenyl)-4*H*-1,2,4-triazol-3-yl)ethan-1-amine Hydrochloride (**53**)

Yield 0.92 g (4%). M.p. 202–210 °C. ¹H NMR (300 MHz, DMSO-*d*₆) δ 8.05 (br.s, 3H), 7.81–7.77 (m, 1H), 7.64 (dd, *J* = 8.0, 1.6 Hz, 1H), 7.54–7.47 (m, 2H), 7.45–7.36 (m, 1H), 7.31–7.24 (m, 1H), 7.21–7.17 (m, 1H), 7.04 (dd, *J* = 8.0, 2.6 Hz, 1H), 3.26–3.15 (m, 2H), 3.11–3.03 (m, 2H). ¹³C NMR (75 MHz, DMSO-*d*₆) δ 157.2, 157.1, 154.4, 151.1, 130.9, 130.7, 129.0, 126.0, 125.0, 121.8, 121.0, 120.9, 118.3, 114.2, 37.1, 24.6. HRMS (ESI) calcd for C₁₆H₁₆ClN₄O [M + H⁺] 315.1007 Da, found 315.1007 Da.

2.2.49. 2-(5-(4-[4-Methylphenoxy]phenyl)-4*H*-1,2,4-triazol-3-yl)ethan-1-amine Hydrochloride (**54**)

Yield 0.03 g (13%). M.p. 234–236 °C. ¹H NMR (300 MHz, DMSO-*d*₆) δ 8.16 (br.s, 3H), 8.06–8.00 (m, 2H), 7.28–7.21 (m, 2H), 7.09–6.96 (m, 4H), 3.30–3.19 (m, 2H), 3.16–3.07 (m, 2H), 2.31 (s, 3H). ¹³C NMR (75 MHz, DMSO-*d*₆) δ 158.9, 156.7, 156.3, 153.3, 133.5, 130.7, 128.1, 122.9, 119.6, 117.9, 37.0, 24.6, 20.4. HRMS (ESI) calcd for C₁₇H₁₉N₄O [M + H⁺] 295.1553 Da, found 295.1553 Da.

2.2.50. 3-(5-(2-Aminoethyl)-4*H*-1,2,4-triazol-3-yl)phenol Hydrochloride (**55**)

Yield 0.022 g (11%). M.p. 234–235 °C. ¹H NMR (300 MHz, DMSO-*d*₆) δ 8.18 (br.s, 3H), 7.50–7.43 (m, 2H), 7.29 (t, *J* = 7.8 Hz, 1H), 6.92–6.86 (m, 1H), 3.31–3.19 (m, 2H), 3.17–3.08 (m, 2H). ¹³C NMR (75 MHz, DMSO-*d*₆) δ 157.8, 157.0, 156.3, 130.1, 129.4, 117.1, 117.0, 113.0, 37.1, 24.6. HRMS (ESI) calcd for C₁₀H₁₃N₄O [M + H⁺] 205.1084 Da, found 205.1084 Da.

2.2.51. 2-(5-(4-[(2-Fluorobenzyl)oxy]-3-iodophenyl)-4*H*-1,2,4-triazol-3-yl)ethan-1-amine Hydrochloride (**56**)

Yield 0.045 g (20%). M.p. 208–209 °C. ¹H NMR (300 MHz, DMSO-*d*₆) δ 8.47–8.44 (m, 1H), 8.14 (br.s, 3H), 8.08–8.00 (m, 1H), 7.71–7.63 (m, 1H), 7.49–7.40 (m, 1H), 7.33–7.24 (m, 3H), 5.30 (s, 2H), 3.30–3.18 (m, 2H), 3.15–3.06 (m, 2H). ¹³C NMR (75 MHz, DMSO-*d*₆) δ 160.5 (d, *J* = 246.2 Hz), 158.0, 156.8, 156.4, 136.7, 130.8 (d, *J* = 7.9 Hz), 130.6, 127.8, 124.8, 124.0, 123.5 (d, *J* = 14.8 Hz), 115.7 (d, *J* = 19.4 Hz), 113.3, 87.3, 65.1, 37.3, 24.8. HRMS (ESI) calcd for C₁₇H₁₇FIN₄O [M + H⁺] 439.0426 Da, found 439.0426 Da.

2.2.52. 4-(5-(2-Aminoethyl)-4*H*-1,2,4-triazol-3-yl)-2-methylphenol Hydrochloride (**57**)

Yield 0.057 g (29%). M.p. 158–160 °C. ¹H NMR (300 MHz, DMSO-*d*₆) δ 8.31 (br.s, 3H), 8.01–7.97 (m, 1H), 7.94–7.88 (m, 1H), 7.03 (d, *J* = 8.4 Hz, 1H), 3.42–3.27 (m, 2H), 3.27–3.19 (m, 2H), 2.17 (s, 3H). ¹³C NMR (75 MHz, DMSO-*d*₆) δ 159.27, 153.66, 153.49, 129.70, 126.46, 125.16, 115.22, 113.84, 36.40, 23.82, 15.99. HRMS (ESI) calcd for C₁₁H₁₅N₄O [M + H⁺] 219.1240 Da, found 219.1240 Da.

2.3. General Procedure 2—Synthesis of Compounds **58–67**

Compound **68** or **69** (2.06 mmol, 1 equiv.) was dissolved in dry tetrahydrofuran (10 mL). Then, 3,4-Dihydro-2*H*-pyran (0.93 mL, 10 mmol, 5 equiv.) and *p*-toluenesulfonic acid (35 mg, 0.21 mmol, 0.1 equiv.) were added and the resulting mixture was heated at reflux for 5 h. The course of the reaction was followed by thin-layer chromatography (eluent—chloroform). On completion, the reaction mixture was cooled to room temperature and partitioned between ethyl acetate (100 mL) and water (50 mL). The organic layer was separated, washed with 5% aq. K₂CO₃ and 3% aq. citric acid, filtered through a plug of anhydrous Na₂SO₄ and concentrated on a rotary evaporator. The yield of the THP protection step was deemed quantitative. The flask with the residue was flushed with argon and the residue (1 mmol) was weighed out, under argon, into an argon filled flask and dissolved in 1,4-dioxane. 20% aq. Na₂CO₃ (3.5 mL) and the respective boronic acid (2 mmol) were added, followed by Pd(PPh₃)₄ (0.03 mmol) and PdCl₂(PPh₃)₂ (0.03 mmol).

The mixture was heated at reflux under argon for 3–4 h while the progress of the reaction was monitored by thin-layer chromatography (eluent—2% methanol in chloroform). On completion, the reaction mixture was cooled to room temperature and partitioned between ethyl acetate (100 mL) and water (50 mL). The organic phase was washed with 5% aq. K_2CO_3 , passed through a plug of anhydrous Na_2SO_4 , and concentrated in vacuo and the residue was treated, fractionated, on silica gel using 50% ethyl acetate in hexane as eluent. Fractions containing the coupling product were pooled and concentrated to dryness. The residue was treated with 4M solution of HCl in 1,4-dioxane (1 h, room temperature). Following concentration on a rotary evaporator, the crystalline residue was triturated with ether and the solids were filtered off, washed with more ether, and air-dried to provide an analytically pure title compound as a crystalline residue.

2.3.1. 2-(5-(4'-Methoxy-(1,1'-biphenyl)-4-yl)-4H-1,2,4-triazol-3-yl)ethan-1-amine Hydrochloride (**58**)

Yield 0.065 g (50%). M.p. 300–301 °C. 1H NMR (300 MHz, $DMSO-d_6$) δ 8.23 (br.s, 3H), 8.13 (d, $J = 8.2$ Hz, 2H), 7.84–7.76 (m, 2H), 7.74–7.67 (m, 2H), 7.05 (d, $J = 8.5$ Hz, 2H), 3.81 (s, 3H), 3.33–3.22 (m, 2H), 3.20–3.12 (m, 2H). ^{13}C NMR (75 MHz, $DMSO-d_6$) δ 159.5, 157.0, 156.6, 141.3, 131.6, 128.0, 126.9, 126.7, 126.6, 114.7, 55.4, 37.2, 24.7. HRMS (ESI) calcd for $C_{17}H_{19}N_4O$ [$M + H^+$] 295.1553 Da, found 295.1553 Da.

2.3.2. 2-(5-(4'-Trifluoromethoxy-(1,1'-biphenyl)-4-yl)-4H-1,2,4-triazol-3-yl)ethan-1-amine Hydrochloride (**59**)

Yield 0.06 g (35%). M.p. 299–300 °C. 1H NMR (300 MHz, $DMSO-d_6$) δ 8.25 (br.s, 3H), 8.17 (d, $J = 8.3$ Hz, 2H), 7.87 (t, $J = 8.1$ Hz, 4H), 7.48 (d, $J = 8.3$ Hz, 2H), 3.34–3.22 (m, 2H), 3.21–3.13 (m, 2H). ^{13}C NMR (75 MHz, $DMSO-d_6$) δ 157.3, 156.6, 148.1, 140.0, 138.7, 128.8, 128.3, 127.5, 126.9, 121.7, 120.3 (d, $J = 256.3$ Hz), 37.2, 24.6. HRMS (ESI) calcd for $C_{17}H_{16}F_3N_4O$ [$M + H^+$] 349.1271 Da, found 349.1271 Da.

2.3.3. 2-(5-(3'-Fluoro-(1,1'-biphenyl)-4-yl)-4H-1,2,4-triazol-3-yl)ethan-1-amine Hydrochloride (**60**)

Yield 0.042 g (26%). M.p. 260–262 °C. 1H NMR (300 MHz, $DMSO-d_6$) δ 8.20 (br.s, 3H), 8.15 (d, $J = 8.2$ Hz, 2H), 7.87 (d, $J = 8.2$ Hz, 2H), 7.67–7.47 (m, 3H), 7.29–7.18 (m, 1H), 3.33–3.21 (m, 2H), 3.19–3.10 (m, 2H). ^{13}C NMR (75 MHz, $DMSO-d_6$) δ 163.1 (d, $J = 243.4$ Hz), 157.4, 156.7, 142.1 (d, $J = 8.0$ Hz), 140.3, 131.4 (d, $J = 8.4$ Hz), 128.7, 127.8, 127.1, 123.2 (d, $J = 2.4$ Hz), 115.1 (d, $J = 21.4$ Hz), 113.9 (d, $J = 22.2$ Hz), 37.4, 25.0. HRMS (ESI) calcd for $C_{16}H_{16}FN_4$ [$M + H^+$] 283.1354 Da, found 283.1354 Da.

2.3.4. 2-(5-(2',4'-Difluoro-(1,1'-biphenyl)-4-yl)-4H-1,2,4-triazol-3-yl)ethan-1-amine Hydrochloride (**61**)

Yield 0.059 g (44%). M.p. 251–253 °C. 1H NMR (300 MHz, $DMSO-d_6$) δ 8.12 (m, 5H), 7.73–7.60 (m, 3H), 7.45–7.34 (m, 1H), 7.29–7.18 (m, 1H), 3.32–3.20 (m, 2H), 3.18–3.09 (m, 2H). ^{13}C NMR (75 MHz, $DMSO-d_6$) (75 MHz, $DMSO$) δ 162.0 (dd, $J = 208.5, 12.3$ Hz), 158.7 (dd, $J = 210.1, 12.4$ Hz), 156.4, 155.7, 135.5, 131.8 (dd, $J = 9.7, 4.6$ Hz), 129.1 (d, $J = 2.7$ Hz), 127.6, 126.2, 123.9 (dd, $J = 13.1, 3.8$ Hz), 112.1 (dd, $J = 21.1, 3.6$ Hz), 104.7 (t, $J = 26.6$ Hz), 36.7, 24.2. HRMS (ESI) calcd for $C_{16}H_{15}F_2N_4$ [$M + H^+$] 301.1259 Da, found 301.1259 Da.

2.3.5. 2-(5-(4'-Chloro-(1,1'-biphenyl)-4-yl)-4H-1,2,4-triazol-3-yl)ethan-1-amine Hydrochloride (**62**, LK00764)

Yield 0.047 g (36%). M.p. 247–249 °C. 1H NMR (300 MHz, $DMSO-d_6$) δ 8.23–8.09 (m, 5H), 7.87–7.74 (m, 4H), 7.58–7.51 (m, 2H), 3.32–3.20 (m, 2H), 3.18–3.09 (m, 2H). ^{13}C NMR (75 MHz, $DMSO-d_6$) δ 157.1, 156.4, 139.1, 138.0, 132.7, 129.0, 128.4, 128.1, 127.0, 126.7, 37.0, 24.6. HRMS (ESI) calcd for $C_{16}H_{16}ClN_4$ [$M + H^+$] 299.1058 Da, found 299.1058 Da.

2.3.6. 2-(5-(3'-Trifluoromethyl-(1,1'-biphenyl)-4-yl)-4H-1,2,4-triazol-3-yl)ethan-1-amine Hydrochloride (**63**)

Yield 0.04 g (27%). M.p. 210–212 °C. ¹H NMR (300 MHz, DMSO-*d*₆) δ 8.27–8.14 (m, 5H), 8.11–8.02 (m, 2H), 7.97–7.89 (m, 2H), 7.81–7.69 (m, 2H), 3.34–3.22 (m, 2H), 3.19–3.11 (m, 2H). ¹³C NMR (75 MHz, DMSO-*d*₆) δ 156.98, 156.29, 140.33, 139.54, 130.83, 130.19, 129.88 (q, J = 31.6 Hz), 128.53, 127.50, 126.75, 124.47 (q, J = 3.5 Hz), 124.22 (q, J = 272.5 Hz), 123.13 (q, J = 3.7 Hz), 36.97, 24.55. HRMS (ESI) calcd for C₁₇H₁₆F₃N₄ [M + H⁺] 333.1322 Da, found 333.1322 Da.

2.3.7. 2-(5-(3',4'-Dimethoxy-(1,1'-biphenyl)-4-yl)-4H-1,2,4-triazol-3-yl)ethan-1-amine Hydrochloride (**64**)

Yield 0.046 g (32%). M.p. 199–201 °C. ¹H NMR (300 MHz, DMSO-*d*₆) δ 8.28 (br.s, 3H), 8.16 (d, J = 8.4 Hz, 2H), 7.84 (d, J = 8.4 Hz, 2H), 7.33–7.27 (m, 2H), 7.08–7.03 (m, 1H), 3.86 (s, 3H), 3.80 (s, 3H), 3.35–3.25 (m, 2H), 3.23–3.16 (m, 2H). ¹³C NMR (75 MHz, DMSO-*d*₆) δ 156.2, 155.9, 149.2, 149.1, 141.8, 131.8, 126.8, 126.7, 125.8, 119.1, 112.3, 110.4, 55.8, 55.7, 36.9, 24.5. HRMS (ESI) calcd for C₁₈H₂₁N₄O₂ [M + H⁺] 325.1659 Da, found 325.1659 Da.

2.3.8. 2-(5-(3',5'-Difluoro-(1,1'-biphenyl)-4-yl)-4H-1,2,4-triazol-3-yl)ethan-1-amine Hydrochloride (**65**)

Yield 0.05 g (38%). M.p. 260–262 °C. ¹H NMR (300 MHz, DMSO-*d*₆) δ 8.32 (br.s, 3H), 8.22–8.17 (m, 2H), 7.95–7.90 (m, 2H), 7.59–7.49 (m, 2H), 7.31–7.22 (m, 1H), 3.35–3.16 (m, 4H). ¹³C NMR (75 MHz, DMSO-*d*₆) δ 162.2 (dd, J = 205.6, 12.3 Hz), 158.9 (dd, J = 207.4, 12.3 Hz), 157.5, 156.3, 135.3, 131.9 (dd, J = 9.7, 4.7 Hz), 129.2 (d, J = 2.9 Hz), 128.5, 126.2, 124.2 (dd, J = 13.3, 3.8 Hz), 112.2 (dd, J = 21.2, 3.6 Hz), 104.6 (dd, J = 26.9, 25.9 Hz), 37.0, 24.6. HRMS (ESI) calcd for C₁₆H₁₅F₂N₄ [M + H⁺] 301.1259 Da, found 301.1259 Da.

2.3.9. 2-(5-(4'-(2',4'-Difluoro-(1,1'-biphenyl)-3-yl)-4H-1,2,4-triazol-3-yl)ethan-1-amine Hydrochloride (**66**)

Yield 0.0262 g (19%). M.p. 255–257 °C. ¹H NMR (300 MHz, DMSO-*d*₆) δ 8.28 (br.s, 3H), 8.23 (s, 1H), 8.14–8.07 (m, 1H), 7.73–7.59 (m, 3H), 7.45–7.35 (m, 1H), 7.28–7.19 (m, 1H), 3.34–3.13 (m, 4H). ¹³C NMR (75 MHz, DMSO-*d*₆) δ 162.1 (dd, J = 211.4, 12.4 Hz), 158.9 (dd, J = 213.0, 12.3 Hz), 157.0, 156.0, 134.9, 132.0 (dd, J = 9.7, 4.6 Hz), 130.2 (d, J = 2.3 Hz), 129.4, 128.9, 126.3 (d, J = 2.3 Hz), 125.6, 124.2 (dd, J = 13.3, 3.8 Hz), 112.2 (dd, J = 21.2, 3.7 Hz), 104.6 (t, J = 26.4 Hz), 36.9, 24.4. HRMS (ESI) calcd for C₁₆H₁₅F₂N₄ [M + H⁺] 301.1259 Da, found 301.1259 Da.

2.3.10. 2-(5-(4'-(Trifluoromethoxy)-(1,1'-biphenyl)-3-yl)-4H-1,2,4-triazol-3-yl)ethan-1-amine Hydrochloride (**67**)

Yield 0.045 g (28%). M.p. 253–257 °C. ¹H NMR (300 MHz, DMSO-*d*₆) δ 8.38–8.35 (m, 1H), 8.18 (br.s, 3H), 8.09–8.04 (m, 1H), 7.91–7.85 (m, 2H), 7.82–7.77 (m, 1H), 7.66–7.59 (m, 1H), 7.53–7.47 (m, 2H), 3.31–3.21 (m, 2H), 3.18–3.11 (m, 2H). ¹³C NMR (75 MHz, DMSO-*d*₆) δ 157.1, 156.5, 148.1 (q, J = 1.7 Hz), 139.4, 138.8, 129.8, 129.4, 128.8, 128.2, 125.5, 124.4, 121.6, 120.2 (q, J = 256.4 Hz), 37.0, 24.6. HRMS (ESI) calcd for C₁₇H₁₆F₃N₄O [M + H⁺] 349.1271 Da, found 349.1271 Da.

2.4. In Silico Modeling

The TAAR1 protein homology model was built with AlphaFold software [17]. The protein model (Q96RJ0) was downloaded from the Uniprot database [18]. The downloaded protein model was preprocessed with the use of a protein preparation wizard, included in Schrodinger Suite (version 2021-4). At this step, we eliminate typical errors in the protein model, such as invalid bond orders, protonation states, atom typing, missing amino acid sidechains, missing loops, clashes between sidechains, incorrect torsions, etc. All manipulations with proteins and ligands were carried out in the OPLS46 force field, used in Schrodinger Suite [19]. The three-dimensional structure of the ligands used for calculations was generated in the same forcefield—OPLS46 [19]. Moreover, for all ligands,

possible protonation states were calculated with the use of the Epik module of Schrodinger Suite [20]. Ligand docking with the prepared TAAR1 protein model was performed with the use of a Glide induced-fit docking (IFD) method [21]. This takes into account protein flexibility in the presence of ligand. The IFD protocol supports direct grid box placement. The grid box for molecular docking was centered on the following TAAR1 residues: D103, I104, S107, V184, F186, T194, F195, F267, F268, I290, and Y294. The grid size is: $16 \times 16 \times 16$ Å. Protein structure refinement during IFD was limited by 6 Å of ligand poses with sidechain optimization. The first docking step generated 20 poses per ligand. For redocking (after protein structure refinement), structures within 30 kcal/mol of the best structure and within the top 15 structures per ligand were selected. The best-fitting binding pose was selected in accordance with docking solutions clustering and interactions with the crucial residues found in literature [9,16,22]. Final prioritization was determined by IFDscore and GlideScore values. The metadynamics calculations protocol was fully automatic: solvent—SPC, automatic counterions addition, system size in accordance to the protein–ligand complex with buffer zone of 10 Å. Equilibration: GCMC Solvate Pocket, μ VT ensemble, $T = 300$ K, restraints on heavy atoms; GCMC Solvate Pocket, μ VT ensemble, $T = 300$ K, no restraints; Brownian Dynamics NVT, $T = 300$ K, small timesteps, and restraints on solute heavy atoms. Main simulation—10 ns, NPT, $T = 300$ K. For each ligand, metadynamics simulation was repeated seven times, which was necessary for statistical weighting. On the basis of molecular metadynamics calculations, the protein–ligand complex stability was evaluated by RMSD value calculation for a ligand near protein. The second value—persistence CompScore, value including protein–ligand interactions, such as π – π stacking, hydrogen bonds, and salt bridges.

2.5. BRET Analysis

The Bioluminescence Resonance Energy Transfer approach (BRET) has been used for functional activity experiments. HEK-293 cells were transiently transfected with cDNA for TAARs and cAMP BRET biosensor (EPAC) and then plated in a 96-well plate, as described [23]. All compounds were tested at the initial concentration of 10 μ M. Then, for active compounds, a concentration-response analysis was performed in order to calculate the EC_{50} values. A natural agonist of TAAR1 β -phenylethylamine (β -PEA) was used as a positive control.

2.6. In Vivo Efficacy Evaluation

2.6.1. Subjects

Drug and test naïve Wistar (3–4 months old in the beginning of experiments) rats were purchased from the State Breeding Farm “Rappolovo” (St. Petersburg, Russia). The recently described dopamine transporter knockout rats (DAT-KOs) were raised in an animal facility of the Valdman Institute of Pharmacology. All rodents were housed under standard laboratory conditions: 12 h light/dark cycle (lights on at 08:00 h) at 21 ± 2 °C and $50 \pm 20\%$ humidity. The rats were housed in groups of three to five in standard T IV cages (Tecniplast, Buguggiate, VA, Italy). During the entire experiment, the rats had free access to filtered (“AQUAPHOR”, Saint Petersburg, Russia) tap water and standard laboratory rat chow (receipt ИК 120-1, KKZ “Laboratorkorm”, Moscow, Russia). All experiments were carried out during the light period of the light/dark cycle after at least one week of habituation to the animal facility. The cages, corn cob bedding (“KKZ “Zolotoy pochatok”” LLC, Voronezh, Russia), and water bottles were changed once a week.

Experimental protocols were approved by the Local Animal Care and Use Committee of First Pavlov State Saint Petersburg Medical University.

2.6.2. Compounds

MK-801 (dizocilpine, (+)-5-methyl-10,11-dihydro-5H-dibenzo-[a,d]-cyclohepten-5,10-imine maleate; Sigma-Aldrich, St. Louis, MO, USA) was dissolved in saline. Compound **62** (LK00764) was dissolved in 10% Tween 80 saline solution. All solutions were made

fresh shortly before injections. Drug doses were tested in a pseudo-random order derived from Latin square design with at least 72 h between consecutive tests. All drugs and vehicles were administered intraperitoneally (i.p.) in the volume of 1 mL/kg. Drug doses are reported as salts. Selection of the MK-801 dose (0.2 mg/kg) was based the previous experience with the compound [24]. All locomotor activity tests (duration—60 min) were performed 15 min after the administration of compounds.

2.6.3. Evaluation of Rat Locomotor Activity Following Drug i.p. Administration

We evaluated locomotor activity of rats in the Actometer apparatus. A detailed description of the apparatus has been presented before [25]. Shortly, each box of the apparatus was equipped by photocell-based infrared sensors to assess horizontal and vertical activity. Wistar rats were tested in the apparatus following a one-week habituation period (baseline period). During this period, the animals were placed in locomotor activity boxes for 60 min per day, 6 days a week to habituate them to the environment. The pharmacological challenge in DAT-KO rats was conducted without habituation to the apparatus.

2.6.4. Stress-Induced Hyperthermia (SIH) Test

SIH test is commonly used to evaluate the potential anti-anxiety effect of drugs [26]. Thermometry was performed rectally in rats with a BIOSEB thermometer. Eight Wistar male rats were injected i.p. with vehicle or LK00764, dissolved in 10% tween 80 saline solution. Latin square design was used for the experiment. The first measurement was performed directly before the injection and the second measurement was performed 15 min later. The difference between the first and the second temperature was calculated.

2.6.5. Statistical Analysis

We used nonparametric statistical methods to analyze the data of the locomotor experiments [25,26]. Alpha was set at 0.05. All statistical analyses were performed using SigmaPlot 12.5 (Systat Software Inc., San Jose, CA, USA). For analysis of the SIH test experiments, Kruskal–Wallis one-way ANOVA was applied.

3. Results and Discussion

3.1. Chemistry

In order to identify new compounds which do not belong to the chemotypes depicted in Figure 1, we performed screening of a focused in-house library of about 1000 compounds comprising various heterocyclic motifs in combination with structural fragments similar to β -PEA or tyramine, well established ligands of TAAR1, as well as other biogenic amine GPCRs. Such a strategy had been reported to deliver higher hit rates in screening a corporate compound collection containing compounds from historic biogenic amine-based drug discovery programs [15]. This hit finding effort identified two submicromolar agonists of TAAR1 (**1** and **2**), both of which displayed a dose-dependent activation of the receptor and were based on the same 2-(4*H*-1,2,4-triazol-3-yl)ethan-1-amine core not previously associated with TAAR1 modulation in the literature (Figure 2).

In order to improve the potency of the newly identified chemotype and possibly understand structure–activity relationships, we performed a massive hit-to-lead analog synthesis by utilizing diversely substituted stock-available (hetero)aromatic carboxylic acid hydrazides **3** and Boc-protected amino amidine building block **4** [27], as depicted in Scheme 1. The three steps were conducted with only one intermittent chromatographic purification after the neat melting of *N*-acyl amidrazone **5**. Thus, the yields of hydrochlorides **6–57** were calculated over the three consecutive steps.

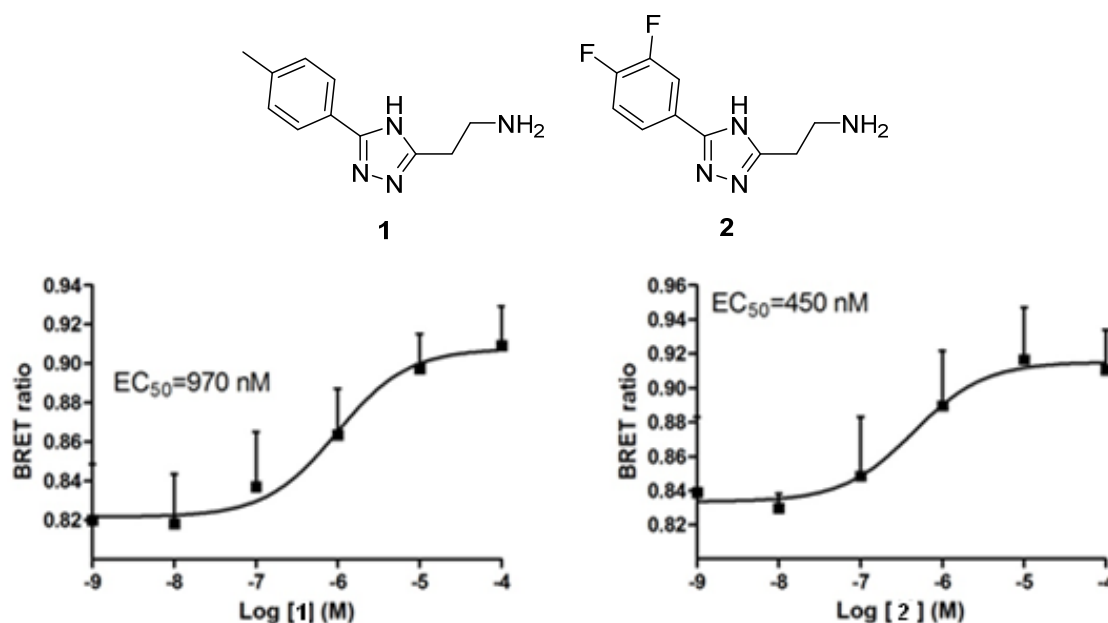
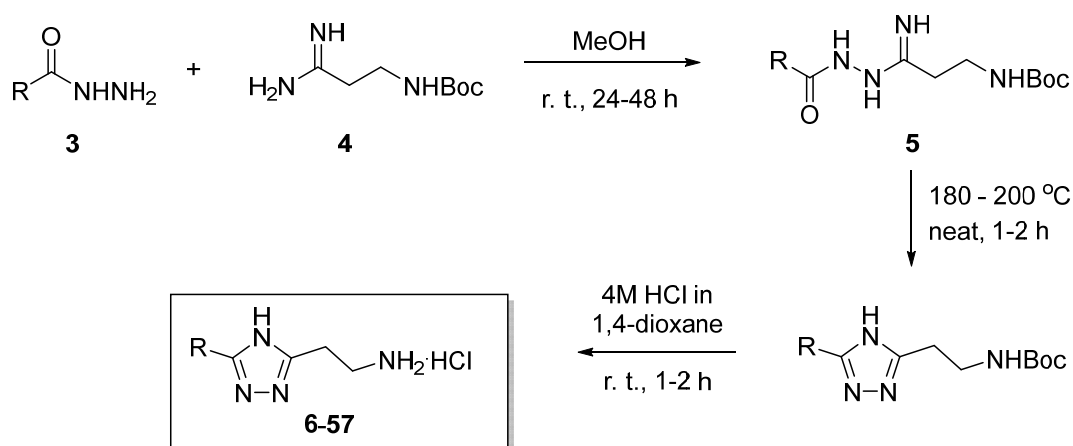
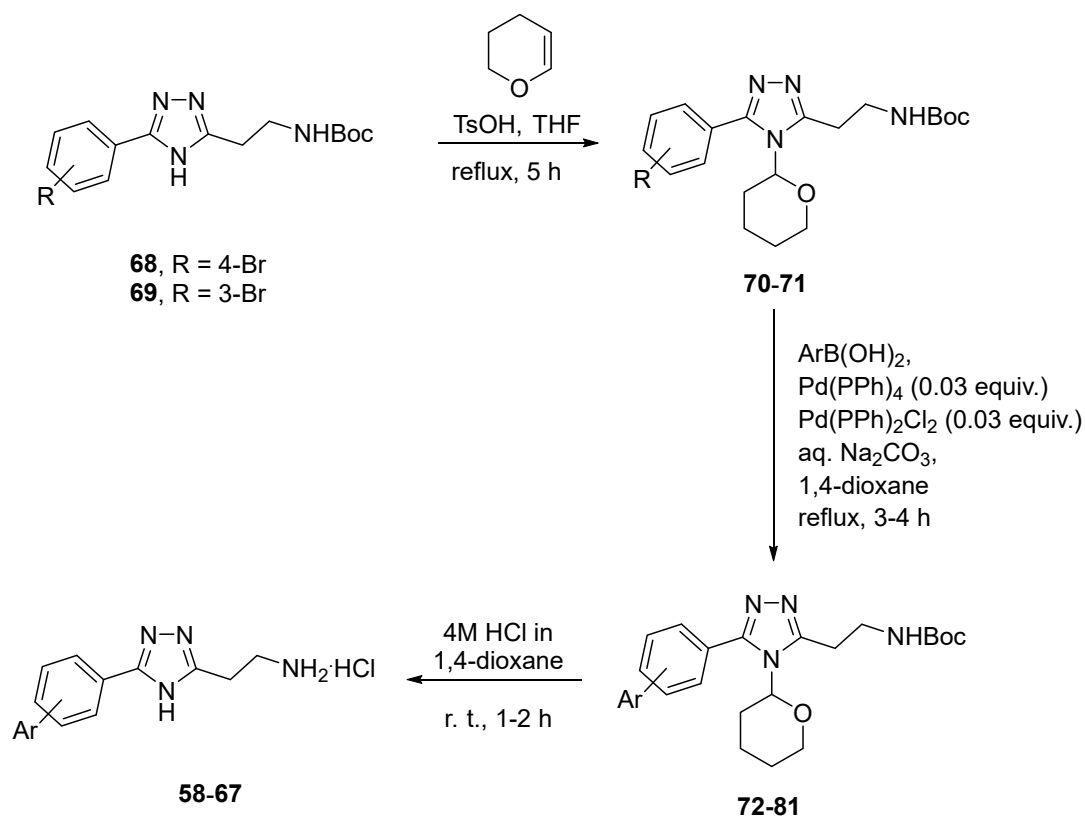


Figure 2. Structures and TAAR1 activation dose–response curves of screening hits 1 and 2 (n = 3).



Scheme 1. Synthesis of 2-(4H-1,2,4-triazol-3-yl)ethan-1-amine analogs 6–57 of the initial hits 1–2.

The resulting 2-(4H-1,2,4-triazol-3-yl)ethan-1-amine analogs 6–57 were tested against TAAR1, as described below. As the TAAR1 activation data for the initial set of compounds (6–57) indicated a clear preference for more lipophilic aromatic substituents on the 1,2,4-triazole core (see discussion in the 3.2. TAAR1 Agonistic Activity section below), we aimed at synthesizing a set of 2-(5-([1,1'-biphenyl]-4-yl)-4H-1,2,4-triazol-3-yl)ethan-1-amines 58–67. For this purpose, Boc-protected 2-(5-(4-bromophenyl)-4H-1,2,4-triazol-3-yl)ethan-1-amine 68 and Boc-protected 2-(5-(3-bromophenyl)-4H-1,2,4-triazol-3-yl)ethan-1-amine 69 were viewed as common precursors which were synthesized on a multigram scale. Unfortunately, application of the standard Suzuki coupling protocol did not lead to appreciable conversion of either 68 or 69 in the attempted coupling. To circumvent this obstacle, the 1,2,4-triazole moiety in these starting materials was protected, with quantitative yield, with the tetrahydropyranyl group [28], and the resulting protected derivatives 70–71 were successfully coupled to a set of boronic acids under mixed Pd(0)/Pd(II) catalysis. Brief chromatographic purification of THP/Boc-protected derivatives 72–73 followed by treatment with 4M HCl in 1,4-dioxane led to simultaneous removal of both protecting groups and afforded biphenyl derivatives 58–67 as hydrochloride salts in modest yields over three steps (Scheme 2). These biphenyl derivatives were also tested for TAAR1 agonism, which led to the discovery of the lead compound in the series (vide infra).



Scheme 2. Synthesis of biphenyl derivatives 58–67.

3.2. TAAR1 Agonistic Activity

Hit expansion compounds 6–57 and 58–67 (see Supplementary Materials for characterization data) were tested for TAAR1 activation using the earlier-developed BRET assay [29]. In addition to EC₅₀ values obtained for each compound, its maximum agonistic effect (E_{max}) was compared to that produced by 1 μM β-phenylethylamine (β-PEA) TAAR1 agonist, employed in this assay as a reference [30]. The data obtained for the initial set of analogs are compiled in Table 1.

Table 1. Agonistic activity of 2-(4H-1,2,4-triazol-3-yl)ethan-1-amine analogs 6–57 of screening hit compounds 1–2 with respect to TAAR1 receptor ^a.

Compound	R	E _{max} ^b	EC ₅₀ (nM)
6		56	>1000
7		132	910
8		108	210
9		116	310

Table 1. Cont.

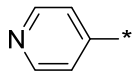
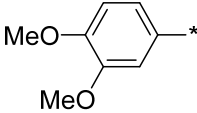
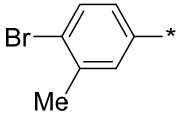
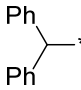
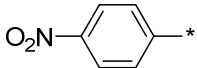
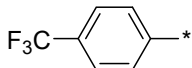
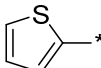
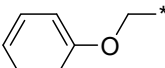
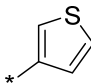
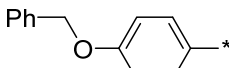
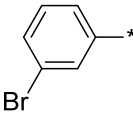
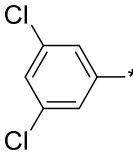
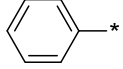
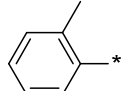
Compound	R	E _{max} ^b	EC ₅₀ (nM)
10		47	>1000
11			inactive
12		87	812
13			inactive
14			inactive
15			inactive
16		138	>1000
17			inactive
18			inactive
19		113	26
20		124	218
21		112	23
22		118	283
23		116	468

Table 1. Cont.

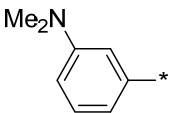
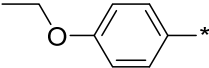
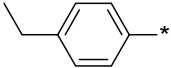
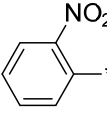
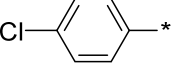
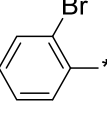
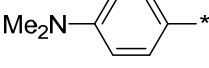
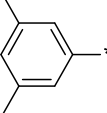
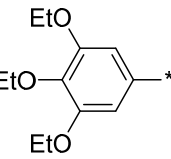
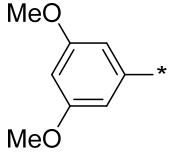
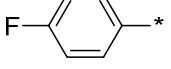
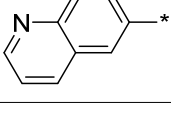
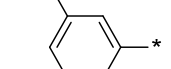
Compound	R	E _{max} ^b	EC ₅₀ (nM)
24			inactive
25		139	550
26		71	>1000
27		69	>1000
28		107	522
29		111	696
30		122	730
31		117	813
32			inactive
33		55	>1000
34		169	>1000
35		41	>1000
36		110	440

Table 1. Cont.

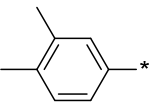
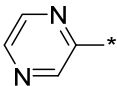
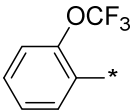
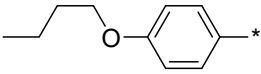
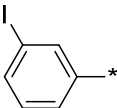
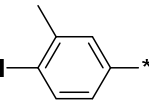
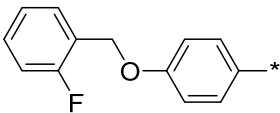
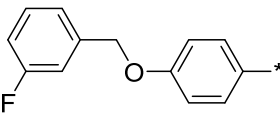
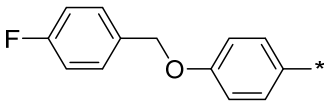
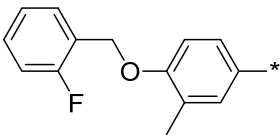
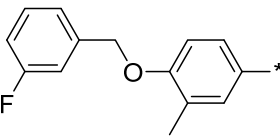
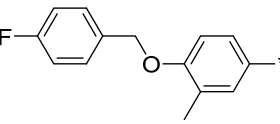
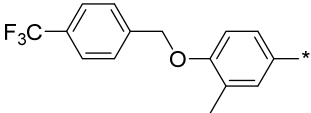
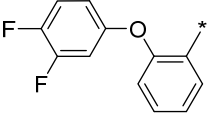
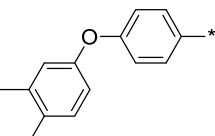
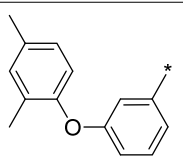
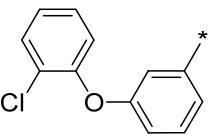
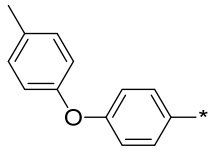
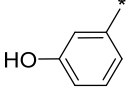
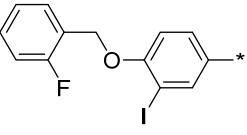
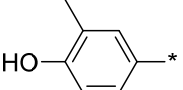
Compound	R	E _{max} ^b	EC ₅₀ (nM)
37		70	>1000
38		inactive	
39		inactive	
40		107	34
41		80	890
42		76	>1000
43		114	45
44		112	30
45		114	22
46		82	398
47		106	142
48		98	163

Table 1. Cont.

Compound	R	E _{max} ^b	EC ₅₀ (nM)
49		inactive	
50		inactive	
51		77	900
52		79	>1000
53		71	847
54		94	150
55		88	>1000
56		87	316
57		90	>1000

^a Mean from 3 different BRET assays (errors were in the range of ± 5 –10% of the reported values). ^b Maximum observed activation of TAAR1 relative to that observed for 1 μ M of β -PEA.

From the examination of the activity data obtained for the unbiased SAR survey set (6–57), it becomes apparent that a simple variation in substituents on the aromatic ring does not lead to substantial improvement in potency. Most of the active compounds manifested themselves as full TAAR1 agonists. Among other things, this initial SAR survey revealed that replacement of the aryl moiety with thienyl (*cf.* 16 and 18) or nitrogen heteroaromatic (*cf.* 10, 35 and 38) as well as highly electron-rich moieties (*cf.* 11, 24, 30, 32) was detrimental to the potency. At the same time, substitution of the benzene ring with lipophilic groups in the *para*-position appears to have a positive effect on the agonistic activity (*cf.* 19, 40, 43–45), which reaches into the double-digit nanomolar range.

Interestingly, the position of the ‘walking fluorine’ in two groups of analogs—**43–45** and **46–48**—has little effect on the potency. However, methyl substitution in the proximal benzene ring (in **46–48**) led to a noticeable drop in the activity. A similar lowering of the activity results from the introduction of iodo substitutions in the phenyl ring (cf. **41–42** and **56**). Introduction of a hydroxy substituent in the phenyl ring (cf. **55** and **57**) completely ablates the agonistic activity.

As hinted at in Section 3.1. Chemistry, above, the latter observation inspired us to explore the rigidified biphenyl versions of the initial hits **58–67**, which were also tested against TAAR1 in BRET assay. The EC₅₀ values obtained for this subset of analogs are compiled in Table 2.

Table 2. Agonistic activity of biphenyl analogs **58–67** of screening hit compounds **1–2** with respect to TAAR1 receptor ^a.

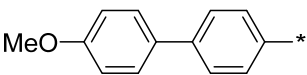
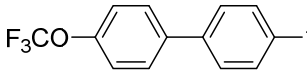
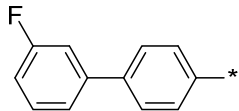
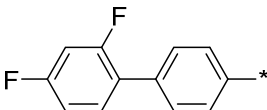
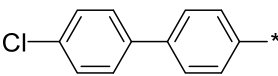
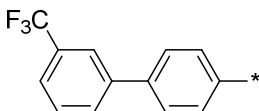
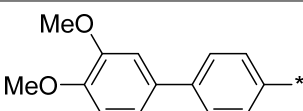
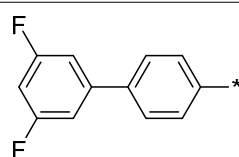
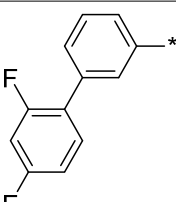
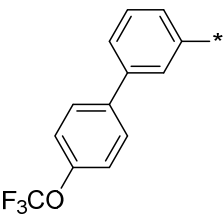
Compound	R	E _{max} ^b	EC ₅₀ (nM)
58		97	6
59		95	13
60		95	26
61		93	18
62 (LK00764)		101	4
63		76	250
64		104	185
65		105	13
66		91	300

Table 2. Cont.

Compound	R	E _{max} ^b	EC ₅₀ (nM)
67		94	96

^a Mean from 3 different BRET assays (errors were in the range of ± 5 –10% of the reported values). ^b Maximum observed activation of TAAR1 relative to that observed for 1 μ M of β -PEA.

The rigidified biphenyl analogs **58**–**67** appeared to display a much better, full agonistic profile with respect to TAAR1. Clearly, the linear *p*-biphenyl versions **58**–**65** were preferred over *m*-biphenyl counterparts **66**–**67**. Simply based on the best potency displayed by compound **62** (LK00764) (its potency (EC₅₀ 4 nM) being more than 30 times higher than that of Ulotaront (EC₅₀ 140 nM) [31], which received FDA Breakthrough Therapy Designation and is currently being investigated in Phase 3 clinical trials [9], it was nominated for further evaluation in rodent pharmacological tests sensitive to TAAR1 agonists [6,7,10,11] and relevant to the development of novel antipsychotics.

3.3. In Silico Modeling

No crystal structure of TAAR1 is available in the Protein Data Bank (PDB). However, modelled structures of TAAR1-interactions obtained by homology modeling can be found in GproteinDb [32]. For instance, a homology model for TAAR1 has been built [9,33] based on the structure of the β 2-adrenergic receptor [34] and used in virtual screening of new TAAR1 ligands [35]. Induced-fit docking of **62** (LK000764) showed a high affinity level of this ligand to TAAR1, which was confirmed by the calculated scoring function values: GScore (kcal/mol): -10.77 ; IFDScore(kcal/mol): -648.38 . The analysis of the binding pose revealed that **62**, in its complex with TAAR1, forms a rich network of lipophilic protein–ligand contacts. The strongest lipophilic contacts were registered in the phenylalanine-rich region of TAAR1: Phe185/186 and Phe195/267/268. This fact was confirmed by the high calculated increment of lipophilic contacts in the scoring function value: -4.27 kcal/mol. The biphenyl moiety of **62** contributes most to these interactions, which is further supported by the π – π stacking interaction with the Phe267 aromatic ring. The other key interaction defining the binding pose is the salt bridge between Asp274 and the protonated amine moiety of **62**, possibly supported by hydrogen bonding to the same Asp274 residue and to the Ile281 backbone residue (Figure 3).

The protein–ligand complex of **62** (LK000764) was tested with the molecular metadynamics method in order to assess molecule retention stability in the TAAR1 active site [36]. The purpose of this method is to evaluate the stability of poses with a Desmond metadynamics [37] molecular dynamics simulation to determine the correctness of the docking pose. The stability was assessed in terms of the fluctuations of the ligand RMSD over the course of the simulation and the persistence of important contacts between the ligand and the receptor (and any other cofactors or solvent molecules) such as hydrogen bonds and π – π interactions. The collective variable for the metadynamics simulation is the ligand RMSD from its initial pose, evaluated after superposition of the binding sites to account for drift. To improve the statistics, multiple simulations were performed, and the results were averaged over the simulations.

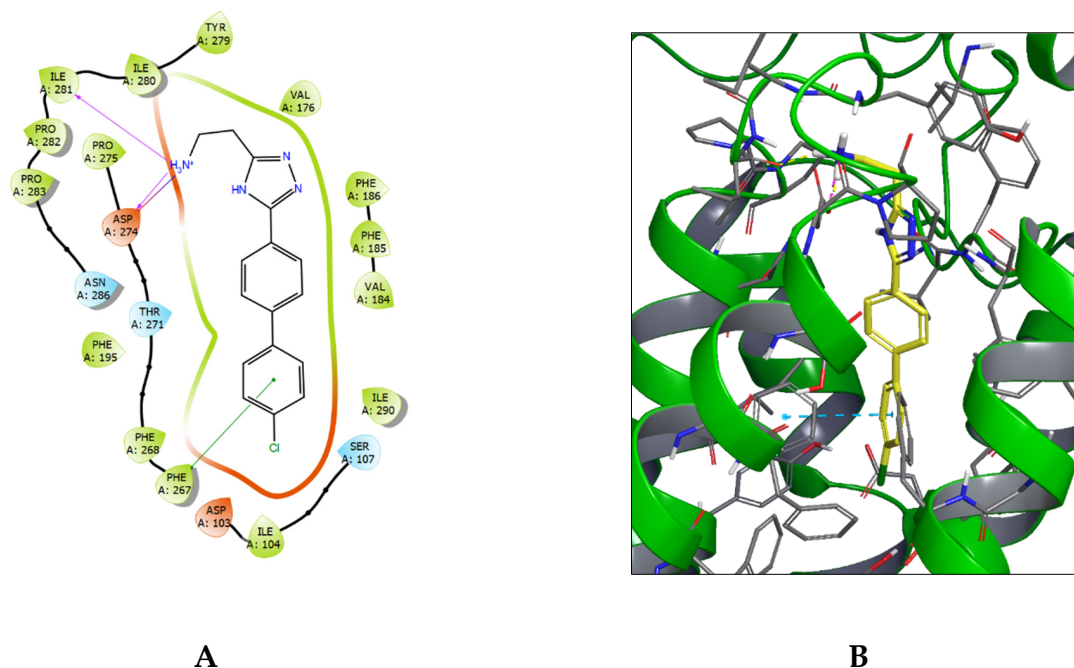


Figure 3. Ligand–protein complex of **62** (LK000764) with TAAR1; (A)—ligand interaction diagram, (B)—ligand positioning in TAAR1 protein structure (blue dashed line— π – π stacking interaction, yellow—hydrogen bond, magenta—salt bridge).

3.4. *In Vivo* Pharmacological Characterization

3.4.1. Effect on MK-801-Induced Hyperactivity and Spontaneous Activity in Rats

Glutamate NMDA receptor antagonist-induced hyperactivity in rodents is commonly used as a pharmacological animal model of schizophrenia in the screening of potential antipsychotics. It is known that the pharmacological activation of TAAR1 is able to decrease NMDA blockers-induced hyperactivity in rodents [8,38]. Thus, we used MK-801 (0.2 mg/kg, i.p.) treatment to induce hyperactivity in rats and analyzed the effects of compound **62** (LK00764) at doses of 0.3, 1, 3, 5, and 10 mg/kg, i.p. on locomotor activity of MK-801-treated Wistar rats.

The Friedman test revealed that pretreatment with compound **62** (LK00764) dose-dependently mitigated MK-801-induced hyperactivity in rats (the main effect of factor ‘dose’ on horizontal activity: $\chi^2 = 11.35$, $df = 5$, $p < 0.05$; on vertical activity: $\chi^2 = 20.47$, $df = 5$, $p < 0.01$). The pairwise comparisons (Dunnett’s test compared with vehicle control treatment) indicated the significant ($p < 0.05$) effect of doses of 5 and 10 mg/kg on both horizontal and vertical locomotor activity (Figure 4A,B).

Next, we analyzed the locomotor effects of compound **62** (LK00764, 0.3–10 mg/kg, i.p.) on the additional group of intact rats ($n = 9$). The administration of compound **62** (LK00764) did not affect horizontal but decreased vertical activity of untreated rats (Figure 5A,B). The Friedmann test demonstrated that the pretreatment with compound **62** (LK00764) did not affect the horizontal activity of Wistar rats (the main effect of the factor ‘dose’: $\chi^2 = 3.63$, $df = 5$, $p = 0.60$) but diminished vertical activity of the animals (the main effect of the factor ‘dose’: $\chi^2 = 27.11$, $df = 5$, $p < 0.001$).

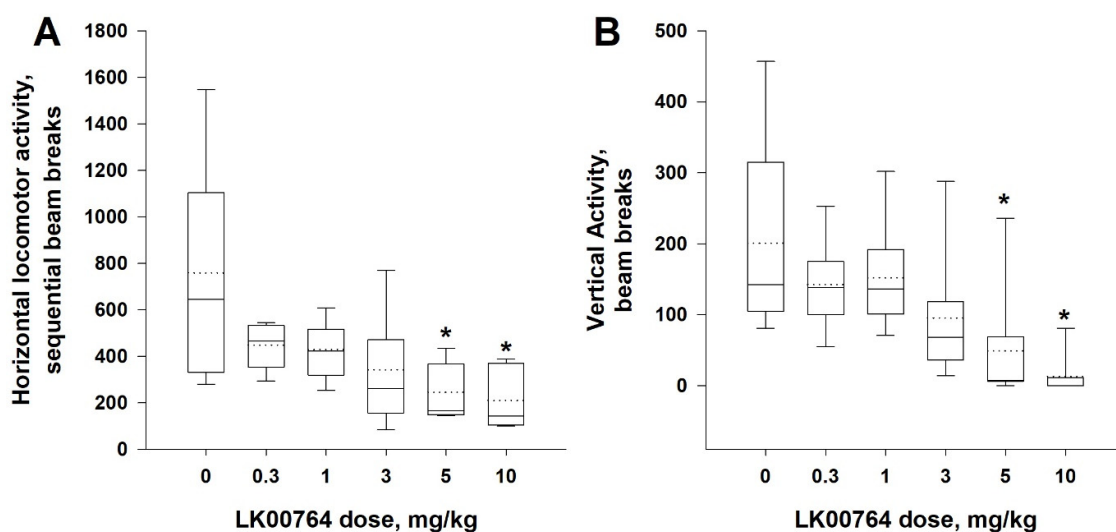


Figure 4. Effect of compound 62 (LK00764) on MK-801-induced hyperactivity. The mitigation action of LK00764 (0.3–10 mg/kg, i.p.) on locomotor hyperactivity following MK-801 (0.2 mg/kg, i.p.) administration in rats (n = 7). (A). Horizontal activity (B). Vertical activity. Data are represented as medians (solid lines), means (dotted lines), and 25th and 75th percentiles in a box-whisker plot, with whiskers indicating 10th and 90th percentiles. * $p < 0.05$ (Dunnett's test) compared with vehicle treatment.

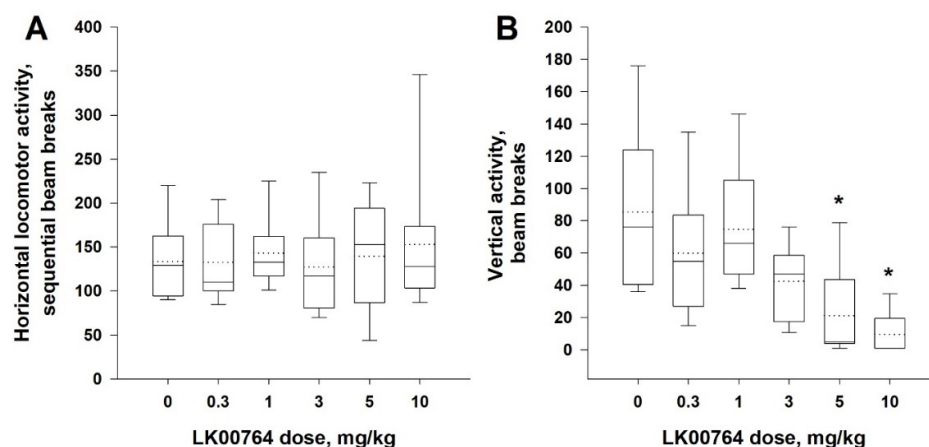


Figure 5. Effect of compound 62 (LK00764) locomotor activity of intact rats. The pretreatment with compound 62 (LK00764, 0.3–10 mg/kg, i.p.) did not affect horizontal (A), but dose-dependently decreased vertical, activity (B) of intact rats. Data are represented as medians (solid lines), means (dotted lines), and 25th and 75th percentiles in a box-whisker plot, with whiskers indicating 10th and 90th percentiles. * $p < 0.05$ (Dunnett's test) compared to the vehicle-treated rats (n = 9).

3.4.2. Effects on Spontaneous Locomotor Hyperactivity of Dopamine Transporter Knockout (DAT-KO) Rats

Animals without DAT have a disrupted re-uptake of dopamine resulting in remarkably elevated extracellular dopamine levels and spontaneous locomotor hyperactivity [39]. Hyperdopaminergic DAT-KO mice and rats are routinely used in search of potential antipsychotic drugs [39,40]. As has been demonstrated in previous studies, TAAR1 agonists are able to mitigate locomotor hyperactivity induced by the lack of DAT [10,38,39]. Thus, we next evaluated the effects of LK00764 (1–10 mg/kg, i.p.) on spontaneous locomotor hyperactivity of DAT-KO rats (n = 9).

We found that the administration of compound 62 (LK00764) was accompanied by a significant dose-dependent decrease in both horizontal (the main effect of the factor 'dose': $\chi^2 = 9.69$, $df = 4$, $p < 0.05$) and vertical (the main effect of the factor 'dose': $\chi^2 = 9.69$, $df = 4$,

$p < 0.05$) activity. The Dunnett's test revealed that only the highest tested dose, 10 mg/kg, significantly ($p < 0.05$) diminished locomotor hyperactivity of the mutants (Figure 6A,B).

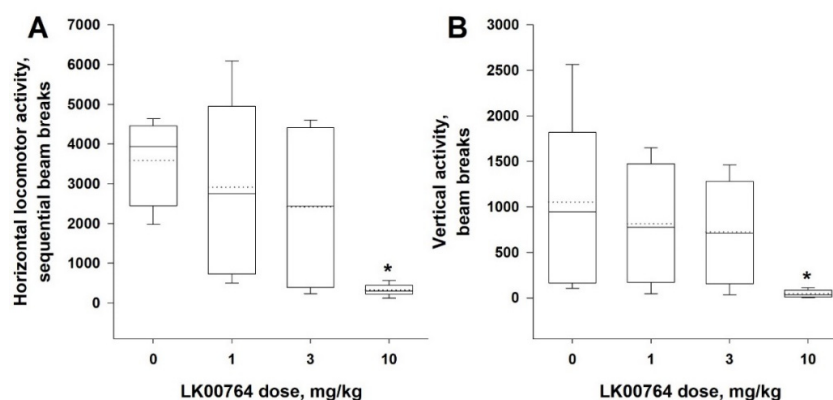


Figure 6. Effect of compound 62 (LK00764) locomotor activity of DAT-KO rats. Administration of compound 62 (LK00764, 1–10 mg/kg, i.p.) decreased both horizontal (A) and vertical activity (B) of DAT-KO rats. Data are represented as medians (solid lines), means (dotted lines), and 25th and 75th percentiles in a box-whisker plot, with whiskers indicating 10th and 90th percentiles. * $p < 0.05$ (Dunnett's test) compared to vehicle-treated rats ($n = 9$ per group).

3.4.3. Effects on Stress-Induced Hyperthermia in Rats

Another behavioral paradigm known to be affected by TAAR1 agonists is the stress-induced hyperthermia test, which is believed to be a sensitive approach to evaluate the anxiolytic action of compounds [10, 42, 39a]. Thus, compound 62 (LK00764) was evaluated in this test at doses of 3 and 5 mg/kg, i.p. (Figure 7). At both doses, this compound was effective in suppressing stress-induced hyperthermia in rats ($p < 0.05$ and $p < 0.001$ for 3 and 5 mg/kg, respectively; Dunn's test).

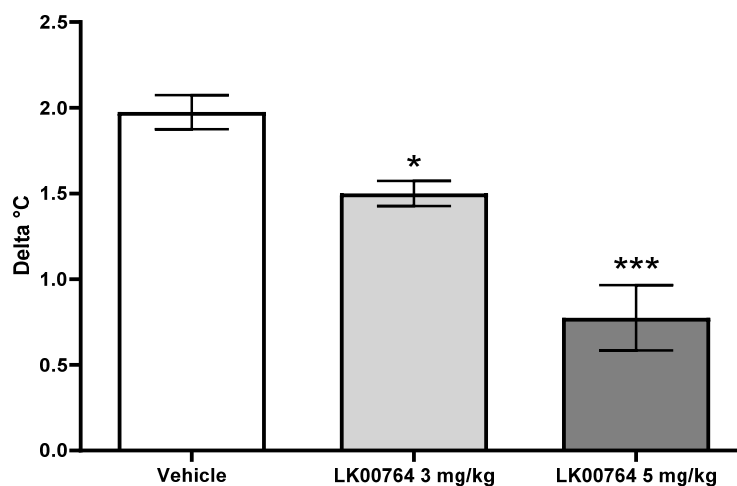


Figure 7. Effect of compound 62 (LK00764) on stress-induced hyperthermia in rats (3 and 5 mg/kg, i.p., $n = 8$ per group); * $p < 0.05$, *** $p < 0.05$, Dunn's test.

4. Conclusions

TAAR1 agonism is emerging as a principally new treatment option for a number of mental conditions, including schizophrenia [7]. Particularly intriguing is the recently demonstrated ability of the TAAR1 agonist Ulotaront to exert potent antipsychotic activity without blocking D₂ dopamine receptors, thereby avoiding common side-effects of D₂ dopamine receptor antagonists [8,9]. Here, we have reported the identification of the novel potent TAAR1 agonist compound 62 (LK00764) with pronounced in vivo activity. Compound 62 (LK00764) demonstrated efficacy in rats through the use of four behavioral

tests typically employed in the screening of antipsychotic drugs and known to demonstrate a response to TAAR1 agonists. Further preclinical studies, including the comparison of the pharmacodynamic effects of compound **62** to those of the most advanced TAAR1 agonists as well as classical antipsychotics, are necessary to evaluate the efficacy, safety, and tolerability of this potent and efficacious TAAR1 agonist for the potential development of this compound as a new pharmacotherapy option for schizophrenia and other psychiatric disorders.

Supplementary Materials: The following supporting information can be downloaded at: <https://www.mdpi.com/article/10.3390/biom12111650/s1>: Copies of ^1H and ^{13}C NMR spectra.

Author Contributions: Conceptualization, M.K. and R.R.G.; methodology, A.L., I.S. and S.K.; validation, I.S., E.V.E. and M.D.; formal analyses, I.S. and K.O.; investigation, A.L., A.S.G., M.D., A.N., A.M. and M.G.; resources, R.R.G. and K.Z.; data curation, I.S., S.K., A.L. and R.R.G.; writing—original draft preparation, M.K.; writing—review and editing, R.R.G.; visualization, S.K. and M.G.; supervision, A.L., S.K., I.S. and R.R.G.; project administration, M.K. and R.R.G.; funding acquisition, R.R.G. and K.Z. All authors have read and agreed to the published version of the manuscript.

Funding: This research was supported by the Russian Science Foundation (grant no. 19-75-30008).

Institutional Review Board Statement: Not applicable.

Informed Consent Statement: Not applicable.

Data Availability Statement: All data are available from the corresponding authors on request.

Acknowledgments: We thank the Research Center for Magnetic Resonance, the Center for Chemical Analysis and Materials Research and Vivarium of Saint Petersburg State University Research Park for obtaining the analytical data.

Conflicts of Interest: The authors declare no conflict of interest.

References

1. Kahn, R.S.; Sommer, I.E.; Murray, R.M.; Meyer-Lindenberg, A.; Weinberger, D.R.; Cannon, T.D.; O'Donovan, M.; Correll, C.U.; Kane, J.M.; van Os, J.; et al. Schizophrenia. *Nat. Rev. Dis. Prim.* **2015**, *1*, 15067. [[CrossRef](#)]
2. Huhn, M.; Nikolakopoulou, A.; Schneider-Thoma, J.; Krause, M.; Samara, M.; Peter, N.; Arndt, T.; Bäckers, L.; Rothe, P.; Cipriani, A.; et al. Comparative efficacy and tolerability of 32 oral antipsychotics for the acute treatment of adults with multi-episode schizophrenia: A systematic review and network meta-analysis. *Lancet* **2019**, *394*, 939–951. [[CrossRef](#)]
3. Lieberman, J.A.; Stroup, T.S.; McEvoy, J.P.; Swartz, M.S.; Rosenheck, R.A.; Perkins, D.O.; Keefe, R.S.; Davis, S.M.; Davis, C.E.; Lebowitz, B.D.; et al. Clinical Antipsychotic Trials of Intervention Effectiveness (CATIE) Investigators. Effectiveness of antipsychotic drugs in patients with chronic schizophrenia. *N. Engl. J. Med.* **2005**, *353*, 1209–1223. [[CrossRef](#)]
4. Borowsky, B.; Adham, N.; Jones, K.A.; Raddatz, R.; Artymyshyn, R.; Ogozalek, K.L.; Durkin, M.M.; Lakhani, P.P.; Bonini, J.A.; Pathirana, S.; et al. Trace amines: Identification of a family of mammalian G protein-coupled receptors. *Proc. Natl. Acad. Sci. USA* **2001**, *98*, 8966–8971. [[CrossRef](#)]
5. Bunzow, J.R.; Sonders, M.S.; Arttamangkul, S.; Harrison, L.M.; Zhang, G.; Quigley, D.I.; Darland, T.; Suchland, K.L.; Pasumamula, S.; Kennedy, J.L.; et al. Amphetamine, 3,4-methylenedioxymethamphetamine, lysergic acid diethylamide, and metabolites of the catecholamine neurotransmitters are agonists of a rat trace amine receptor. *Mol. Pharmacol.* **2001**, *60*, 1181–1188. [[CrossRef](#)]
6. Gainetdinov, R.R.; Hoener, M.C.; Berry, M.D. Trace Amines and Their Receptors. *Pharmacol. Rev.* **2018**, *70*, 549–620. [[CrossRef](#)]
7. Berry, M.D.; Gainetdinov, R.R.; Hoener, M.C.; Shahid, M. Pharmacology of human trace amine-associated receptors: Therapeutic opportunities and challenges. *Pharmacol. Ther.* **2017**, *180*, 161–180. [[CrossRef](#)]
8. Dedic, N.; Dworak, H.; Zeni, C.; Rutigliano, G.; Howes, O.D. Therapeutic potential of TAAR1 agonists in schizophrenia: Evidence from preclinical models and clinical studies. *Int. J. Mol. Sci.* **2021**, *22*, 13185. [[CrossRef](#)]
9. Heffernan, M.L.R.; Herman, L.W.; Brown, S.; Jones, P.G.; Shao, L.; Hewitt, M.C.; Campbell, J.E.; Dedic, N.; Hopkins, S.C.; Koblan, K.S.; et al. Ulotaront: A TAAR1 Agonist for the Treatment of Schizophrenia. *ACS Med. Chem. Lett.* **2021**, *13*, 92–98. [[CrossRef](#)]
10. Revel, F.G.; Moreau, J.L.; Gainetdinov, R.R.; Ferragud, A.; Velázquez-Sánchez, C.; Sotnikova, T.D.; Morairty, S.R.; Harmeyer, A.; Groebke Zbinden, K.; Norcross, R.D.; et al. Trace amine-associated receptor 1 partial agonism reveals novel paradigm for neuropsychiatric therapeutics. *Biol. Psychiatry* **2012**, *72*, 934–942. [[CrossRef](#)] [[PubMed](#)]

11. Revel, F.G.; Moreau, J.-L.; Pouzet, B.; Mory, R.; Bradaia, A.; Buchy, D.; Metzler, V.; Chaboz, S.; Groebke Zbinden, K.; Galley, G.; et al. A new perspective for schizophrenia: TAAR1 agonists reveal antipsychotic- and antidepressant-like activity, improve cognition and control body weight. *Mol. Psychiatry* **2013**, *18*, 543–556. [[CrossRef](#)] [[PubMed](#)]
12. Liu, J.; Wu, R.; Li, J.X. TAAR1 and Psychostimulant Addiction. *Cell. Mol. Neurobiol.* **2020**, *40*, 229–238. [[CrossRef](#)] [[PubMed](#)]
13. Sukhanov, I.; Dorotenko, A.; Dolgorukova, A.; Hoener, M.C.; Gainetdinov, R.R.; Beshpalov, A.Y. Activation of trace amine-associated receptor 1 attenuates schedule-induced polydipsia in rats. *Neuropharmacology* **2019**, *144*, 184–192. [[CrossRef](#)] [[PubMed](#)]
14. Galley, G.; Stalder, H.; Goergler, A.; Hoener, M.C.; Norcross, R.D. Optimisation of imidazole compounds as selective TAAR1 agonists: Discovery of RO5073012. *Bioorg. Med. Chem. Lett.* **2012**, *22*, 5244–5248. [[CrossRef](#)]
15. Galley, G.; Beurier, A.; Décoret, G.; Goergler, A.; Hutter, R.; Mohr, S.; Pähler, A.; Schmid, P.; Türck, D.; Unger, R.; et al. Discovery and Characterization of 2-Amino-oxazolines as Highly Potent, Selective, and Orally Active TAAR1 Agonists. *ACS Med. Chem. Lett.* **2015**, *7*, 192–197. [[CrossRef](#)]
16. Guariento, S.; Tonelli, M.; Espinoza, S.; Gerasimov, A.S.; Gainetdinov, R.R.; Cichero, E. Rational design, chemical synthesis and biological evaluation of novel biguanides exploring species-specificity responsiveness of TAAR1 agonists. *Eur. J. Med. Chem.* **2018**, *146*, 171–184. [[CrossRef](#)]
17. Jumper, J.; Evans, R.; Pritzel, A.; Green, T.; Figurnov, M.; Ronneberger, O.; Tunyasuvunakool, K.; Bates, R.; Židek, A.; Potapenko, A.; et al. Highly accurate protein structure prediction with AlphaFold. *Nature* **2021**, *596*, 583–589. [[CrossRef](#)]
18. The UniProt Consortium. UniProt: The universal protein knowledgebase. *Nucleic Acids Res.* **2017**, *45*, D158–D169. [[CrossRef](#)]
19. Lu, C.; Wu, C.; Ghoreishi, D.; Chen, W.; Wang, L.; Damm, W.; Ross, G.A.; Dahlgren, M.K.; Russel, E.; Von Bargen, C.D.; et al. OPLS4: Improving Force Field Accuracy on Challenging Regimes of Chemical Space. *J. Chem. Theory Comput.* **2021**, *17*, 4291–4300. [[CrossRef](#)]
20. Greenwood, J.R.; Calkins, D.; Sullivan, A.P.; Shelley, J.C. Towards the comprehensive, rapid, and accurate prediction of the favorable tautomeric states of drug-like molecules in aqueous solution. *J. Comput. Aided Mol. Des.* **2010**, *24*, 591–604. [[CrossRef](#)]
21. Repasky, M.P.; Shelley, M.; Friesner, R.A. Flexible ligand docking with Glide. *Curr. Protoc. Bioinform.* **2007**, *18*, 8–12. [[CrossRef](#)]
22. Tonelli, M.; Espinoza, S.; Gainetdinov, R.R.; Cichero, E. Novel biguanide-based derivatives scouted as TAAR1 agonists: Synthesis, biological evaluation, ADME prediction and molecular docking studies. *Eur. J. Med. Chem.* **2017**, *127*, 781–792. [[CrossRef](#)] [[PubMed](#)]
23. Espinoza, S.; Salahpour, A.; Masri, B.; Sotnikova, T.D.; Messa, M.; Barak, L.S.; Caron, M.G.; Gainetdinov, R.R. Functional interaction between Trace Amine Associated Receptor 1 (TAAR1) and dopamine D2 receptor. *Mol. Pharmacol.* **2011**, *80*, 416–425. [[CrossRef](#)] [[PubMed](#)]
24. Sukhanov, I.M.; Zakharaeva, E.S.; Danysz, W.; Beshpalov, A.Y. Effects of NMDA receptor channel blockers, MK-801 and memantine, on locomotor activity and tolerance to delay of reward in Wistar-Kyoto and spontaneously hypertensive rats. *Behav. Pharmacol.* **2004**, *15*, 263–271. [[CrossRef](#)]
25. Sukhanov, I.; Dorofeikova, M.; Dolgorukova, A.; Dorotenko, A.; Gainetdinov, R.R. Trace amine-associated receptor 1 modulates the locomotor and sensitization effects of nicotine. *Front. Pharmacol.* **2018**, *9*, 329. [[CrossRef](#)]
26. Olivier, B.; Zethof, T.; Pattij, T.; van Boogaert, M.; van Oorschot, R.; Leahy, C.; Oosting, R.; Bouwknecht, A.; Veening, J.; van der Gugten, J.; et al. Stress-induced hyperthermia and anxiety: Pharmacological validation. *Eur. J. Pharmacol.* **2003**, *463*, 117–132. [[CrossRef](#)]
27. Barker, P.L.; Gendler, P.L.; Rapoport, H. Acylation of Dibasic Compounds Containing Amino Amidine and Aminoguanidine Functions. *J. Org. Chem.* **1981**, *46*, 2455–2465. [[CrossRef](#)]
28. Riggs, J.R.; Nagy, M.; Elsner, J.; Erdman, P.; Cashion, D.; Robinson, D.; Harris, R.; Huang, D.; Tehrani, L.; Deyanat-Yazdi, G.; et al. The Discovery of a Dual TTK Protein Kinase/CDC2-Like Kinase (CLK2) Inhibitor for the Treatment of Triple Negative Breast Cancer Initiated from a Phenotypic Screen. *J. Med. Chem.* **2017**, *60*, 8989–9002. [[CrossRef](#)]
29. Barak, L.S.; Salahpour, A.; Zhang, X.; Masri, B.; Sotnikova, T.D.; Ramsey, A.J.; Violin, J.D.; Lefkowitz, R.J.; Caron, M.G.; Gainetdinov, R.R. Pharmacological Characterization of Membrane-Expressed Human Trace Amine-Associated Receptor 1 (TAAR1) by a Bioluminescence Resonance Energy Transfer cAMP Biosensor. *Mol. Pharmacol.* **2008**, *74*, 585–594. [[CrossRef](#)]
30. Francesconi, V.; Cichero, E.; Kanov, E.V.; Laurini, E.; Pricl, S.; Gainetdinov, R.R.; Tonelli, M. Novel 1-Amidino-4-Phenylpiperazines as Potent Agonists at Human TAAR1 Receptor: Rational Design, Synthesis, Biological Evaluation and Molecular Docking Studies. *Pharmaceuticals* **2020**, *13*, 391. [[CrossRef](#)]
31. Dedic, N.; Jones, P.G.; Hopkins, S.C.; Lew, R.; Shao, L.; Campbell, J.E.; Spear, K.L.; Large, T.H.; Campbell, U.C.; Hanania, T.; et al. SEP-363856, a Novel Psychotropic Agent with a Unique, Non-D2 Receptor Mechanism of Action. *J. Pharmacol. Exp. Ther.* **2019**, *371*, 1–14. [[CrossRef](#)]
32. Pándy-Szekeres, G.; Esguerra, M.; Hauser, A.S.; Caroli, J.; Munk, C.; Pilger, S.; Keserű, G.M.; Kooistra, A.J.; Gloriam, D.E. The G protein database, GproteinDb. *Nucleic Acids Res.* **2022**, *50*, D518–D525. [[CrossRef](#)]
33. Cichero, E.; Espinoza, S.; Gainetdinov, R.R.; Brasili, L.; Fossa, P. Insights into the Structure and Pharmacology of the Human Trace Amine-Associated Receptor 1 (hTAAR1): Homology Modelling and Docking Studies. *Chem. Biol. Drug Des.* **2013**, *81*, 509–516. [[CrossRef](#)]
34. Rasmussen, S.G.F.; DeVree, B.T.; Zou, Y.; Kruse, A.C.; Chung, K.Y.; Kobilka, T.S.; Thian, F.S.; Chae, P.C.; Pardon, E.; Calinski, D.; et al. Crystal structure of the β_2 adrenergic receptor–Gs protein complex. *Nature* **2011**, *477*, 549–555. [[CrossRef](#)] [[PubMed](#)]

35. Cichero, E.; Espinoza, S.; Franchini, S.; Guariento, S.; Brasili, L.; Gainetdinov, R.R.; Fossa, P. Further insights into the pharmacology of the human trace amine-associated receptors: Discovery of novel ligands for TAAR1 by a virtual screening approach. *Chem. Biol. Drug Des.* **2014**, *84*, 712–720. [[CrossRef](#)]
36. Fusano, L.; Palmer, D.S.; Somers, D.O.; Wall, I.D. Exploring Ligand Stability in Protein Crystal Structures Using Binding Pose Metadynamics. *J. Chem. Inf. Model.* **2020**, *60*, 1528–1539. [[CrossRef](#)] [[PubMed](#)]
37. Barducci, A.; Bonomi, M.; Parrinello, M. Metadynamics. *WIREs Comput. Mol. Sci.* **2011**, *1*, 826–843. [[CrossRef](#)]
38. Revel, F.G.; Moreau, J.-L.; Gainetdinov, R.R.; Bradaia, A.; Sotnikova, T.D.; Mory, R.; Durkin, S.; Groebke Zbinden, K.; Norcross, R.; Meyer, C.A.; et al. TAAR1 activation modulates monoaminergic neurotransmission, preventing hyperdopaminergic and hypoglutamatergic activity. *Proc. Natl. Acad. Sci. USA* **2011**, *108*, 8485–8490. [[CrossRef](#)]
39. Leo, D.; Sukhanov, I.; Zoratto, F.; Illiano, P.; Caffino, S.F.; Messa, G.; Emanuele, M.; Esposito, A.; Dorofeikova, M.; Budygin, E.A.; et al. Pronounced Hyperactivity, Cognitive Dysfunctions, and BDNF Dysregulation in Dopamine Transporter Knock-out Rats. *J. Neurosci.* **2018**, *38*, 1959–1972. [[CrossRef](#)]
40. Efimova, E.V.; Gainetdinov, R.R.; Budygin, E.A.; Sotnikova, T.D. Dopamine transporter mutant animals: A translational perspective. *J. Neurogenet.* **2016**, *30*, 5–15. [[CrossRef](#)] [[PubMed](#)]